Table 1 The clinical findings of the 52 patients with acute exacerbation of idiopathic pulmonary fibrosis on admission

Characteristic	Data
Patient, No. (male/female)	52 (38/14)
Age, years old, mean (range)	71.1 (47–86)
Smoking (current/former/never)	9/22/21
Symptoms	
Dyspnea	52 (100%)
Cough	41 (78.8%)
Fever	22 (42.3%)
Hemoptysis	2 (3.8%)
Comorbidities	
Diabetes	18 (34.6%)
Chronic heart failure	12 (23.1%)
Cancer	7 (13.5%)
Pulmonary hypertension	1 (1.9%)
Prior treatment(s)	
Corticosteroid monotherapy	13 (25.0%)
Corticosteroid plus immunosuppressive agent	12 (23.1%)
Pirfenidone	5 (9.6%)
Home oxygen therapy	15 (28.8%)
Blood sample findings	
WBC, /μl, mean (range)	11434 (4000–21300)
CRP, mg/dl, mean (range)	9.36 (0.1-25.9)
LDH, IU/L, mean (range)	479.2 (138–4135)
KL-6, U/ml, mean (range)	1855 (507–7280)
SP-D, ng/ml, mean (range)	545 (144–2500)

Data are presented as the n and means.

the development of dyspnea within 30 days and were hospitalized at the time of death. A large majority of patients experienced acute episodes of AE-IPF, including 41 (78.8%) patients with coughing and 22 (42.3%) patients with a fever. Only one patient was diagnosed with pulmonary hypertension prior to AE-IPF, whereas 12 patients were additionally diagnosed with pulmonary hypertension at the onset of AE-IPF based on the findings of right heart catheterization and/or transthoracic echocardiography [18]. The median survival period for the patients with AE-IPF was approximately 29 days (range: 1 to 134 days) from admission.

Nearly half of the patients had received corticosteroid therapy before AE-IPF. The therapeutic regimens for AE-IPF are shown in Table 2. Forty-five (86.5%) patients had received high-dose corticosteroid therapy, 43 (82.7%) had received antibacterial drugs and 27 (51.9%) were on mechanical ventilation due to hypoxemia. Sulfamethoxazole/trimethoprim was used to prevent pneumocystis pneumonia in 21 (40.4%) patients. Six (11.5%) patients developed pneumothorax prior to death and 26 (57.8%) developed insulin-dependent diabetes after receiving high-dose corticosteroid therapy.

Table 2 The therapeutic regimen use for the AE-IPF

Treatment	No. (%)
High-dose corticosteroids	45 (86.5)
Immunosuppressive agents	15 (28.8)
Sivelestat sodium	17 (32.7)
PMX-DHP	7 (13.5)
Anticoagulant therapy	12 (23.1)
Mechanical ventilation	27 (51.9)
NPPV	4 (7.7)
Antibacterial drug	43 (82.7)
Carbapenems	15 (28.8)
Quinolones	12 (23.1)
Penicillin-based drugs	4 (7.7)
Cephems	5 (9.6)
Others	7 (13.5)

Abbreviations: AE-IPF Acute exacerbation of idiopathic pulmonary fibrosis, *PMX-DHP* Polymyxin-B direct hemoperfusion, *NPPV* Noninvasive positive pressure ventilation.

Pathological findings

The mean duration between death and autopsy was 286 minutes (range: 60 to 990 minutes). Overall, the median weights of the right and left lungs were 658 g (range: 320 to 1,330 g) and 552 g (range: 260 to 1,000 g), respectively. These median weights were remarkably heavier than the standard lung weights reported for Japanese males (right and left lung weights: 474 and 404 g, respectively) [19]. The underlying pulmonary fibrotic lesion was classified as exhibiting the UIP pattern in all cases. Forty-one (78.8%) patients had DAD (Figure 1A-D), 15 (28.8%) patients had pulmonary hemorrhage (Figure 2A), nine (17.3%) patients had pulmonary thromboembolism (Figure 2B) and six (11.5%) patients had lung carcinoma (Table 3). Only two of the 15 AE-IPF patients with pulmonary hemorrhage received anticoagulant therapy.

The pathological findings in the 11 patients with AE-IPF who met the 2007 criteria but did not have DAD were indicative of UIP alone (n = 5), alveolar hemorrhage (n = 3), pulmonary thromboembolism (n = 1), OP (n = 1) and lung adenocarcinoma (n = 1) (Figure 3). There were no significant differences in any of the patient characteristics between the UIP with DAD and UIP without DAD groups on admission. In addition, there were no correlations or significant differences between the degree of pulmonary hypertension and histological variation. Among the 52 patients with AE-IPF, 13 (25.0%) exhibited gastrointestinal hemorrhage and 18 (34.6%) displayed right ventricular hypertrophy (Figure 2C) as extrapulmonary findings.

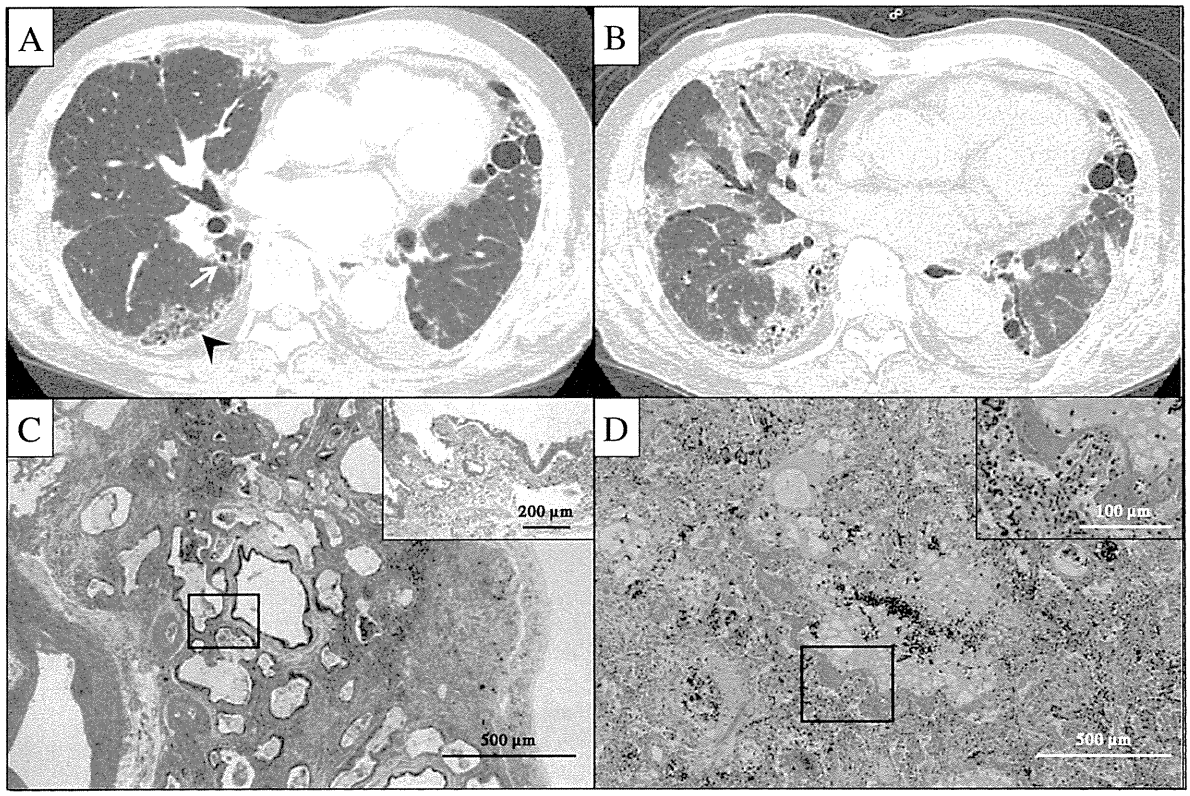

Figure 1 A 78-year-old male with acute exacerbation of idiopathic pulmonary fibrosis (AE-IPF). High resolution computed tomography (HRCT) images at the initial diagnosis of IPF showed subpleural-predominant interstitial fibrosis, traction bronchiectasis (arrow) and honeycombing (arrowhead) **(A)**. HRCT images at the onset of acute exacerbation (12 months after the initial diagnosis) showed diffuse areas of ground glass attenuations superimposed on underlying fibrotic opacities **(B)**. The underling fibrotic lesions were classified as the UIP pattern, including dense interstitial fibrosis with focal squamous or bronchial metaplasia (inset), alternating with only bland-looking alveolar walls (H&E, ×100) **(C)**. DAD with hyaline membranes (inset) superimposed on a background fibrotic and edematous lung with several fibroblastic foci (H&E, ×100) **(D)**.

Infectious causes

Of the 52 autopsies performed, death was attributed to bronchopneumonia in 15 (28.8%) patients (Table 4). In these cases, the pulmonary infectious lesions were not diagnosed until autopsy. The causes of infection included fungal infection in seven cases (13.5%), CMV infection (Figure 2D) in six cases (11.5%) and bacterial infection in five cases (9.6%). One patient with pulmonary aspergillosis died on the first day after AE-IPF; however, the post-mortem pathological findings of the lungs in this case primarily showed a DAD pattern, with only slight bronchopneumonia induced by aspergillosis. Gram staining demonstrated the infectious bacteria to be Gram-negative rods and Gram-positive cocci. Pneumocystis pneumonia was not detected in any patient in the present study. All patients with AE-IPF, except one, had received high-dose corticosteroid therapy and/or immunosuppressive agents. There were also no significant differences in the time interval between the diagnosis of AE-IPF and death based on whether the patient was diagnosed with infectious disease (29.8 vs 31.1 days, p = 0.87).

Discussion

In this study, we retrospectively analyzed the autopsy findings of AE-IPF and clarified that AE-IPF exhibits a variety of pathological findings in addition to DAD. Moreover, the AE-IPF patients were diagnosed with various infectious diseases and complications during their clinical course after AE-IPF.

DAD has been reported to be the focal pathological finding of AE-IPF [9]. DAD also accounted for many cases of AE-IPF in the present investigation, involving a mixture of pulmonary hemorrhage, pulmonary thromboembolism and OP. However, DAD was not observed in all cases. In particular, pulmonary hemorrhage was a representative pathological finding in the AE-IPF patients without DAD. Pulmonary hemorrhage is rarely encountered during the course of IPF [20-22], and it is difficult to make a

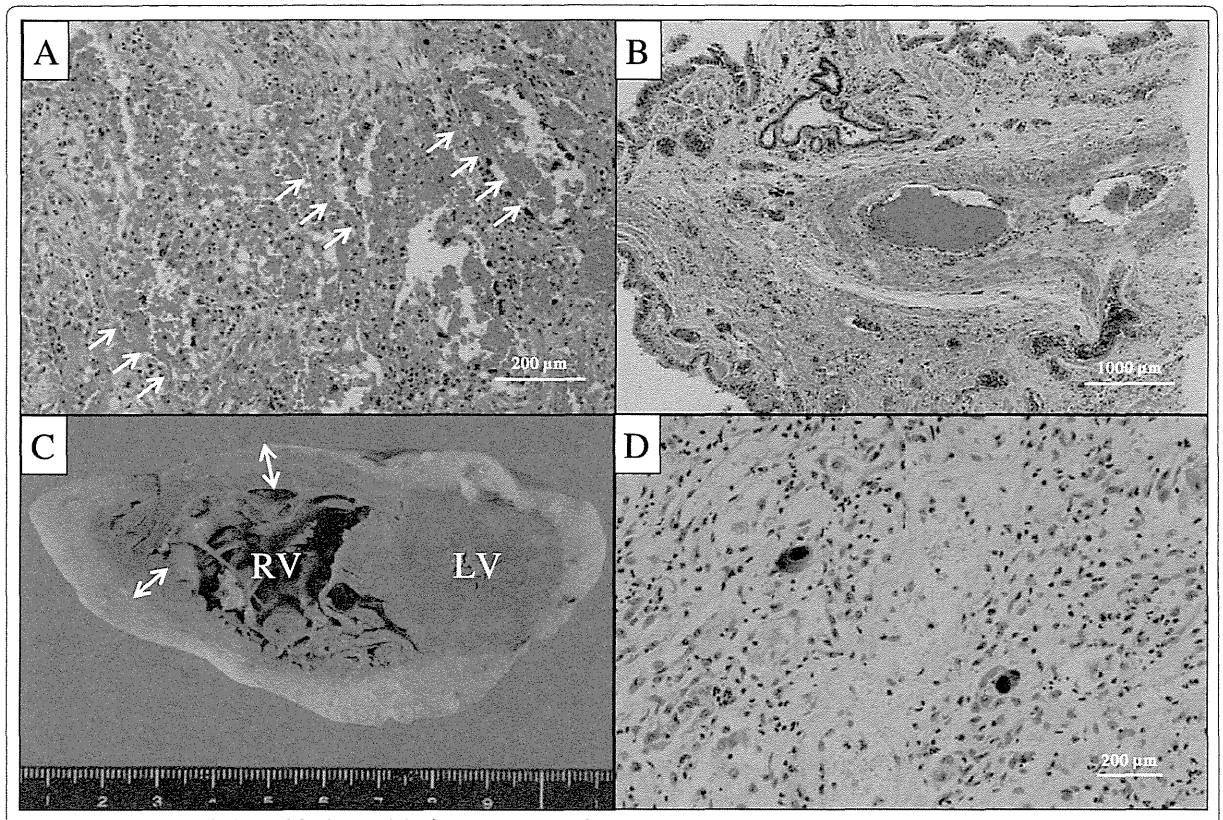

Figure 2 The histopathological findings of the lung specimens obtained at autopsy. The microscopic findings of the lung showed diffuse alveolar hemorrhage (arrows) without any specific evidence of vasculitis **(A)** or pulmonary thromboembolism **(B)** (H&E, ×10). The macroscopic findings of the heart showed overt right ventricular hypertrophy, confirmed by an increased (≥5 mm) right ventricular wall thickness (double-headed arrows) **(C)**. Immunohistochemical staining of an inflamed lung tissue specimen revealed a number of specific cytomegalovirus-positive cells (proliferating type II pneumocytes) **(D)**.

Table 3 The autopsy findings of patients with AE-IPF

Pathological findings	No. (%)
UIP pattern	52 (100)
Diffuse alveolar damage	41 (78.8)
Alveolar hemorrhage	15 (28.8)
Organizing pneumonia	1 (1.9)
Pulmonary thromboembolism	9 (17.3)
Lung cancer	6 (11.5)
Bronchopneumonia	15 (28.8)
Bacterial infection	6 (11.5)
Fungal infection	7 (13.5)
Cytomegalovirus infection	6 (11.5)
Extrapulmonary findings	
Gastrointestinal hemorrhage	13 (25.0)
Right ventricular hypertrophy	18 (34.6)

Abbreviations: AE-IPF Acute exacerbation of idiopathic pulmonary fibrosis, *UIP* Usual interstitial pneumonia.

premortem diagnosis in actual clinical practice without performing BAL. Nevertheless, careful attention is required in such cases, as the use of BAL in IPF patients may increase the risk of acute exacerbation [23]. Moreover, pulmonary thromboembolism frequently occurs as a complication during the course of IPF [24] and can be an important differential diagnosis of AE-IPF.

Regarding acute respiratory distress syndrome (ARDS), in which the diagnostic criteria are based on clinical findings, in the same manner as AE-IPF, Patel S.R. et al. reported that they investigated the pathological findings of 57 cases satisfying the diagnostic criteria for ARDS via open-lung biopsy, with DAD observed in 23 patients (40.3%) [25]. On the other hand, another study reported specific infections in eight patients (14.0%), diffuse alveolar hemorrhage in five patients (8.8%) and bronchiolitis obliterans organizing pneumonia in five patients (8.8%). Moreover, Esteban A. et al. found that, although DAD was observed in 112 of 127 autopsy cases satisfying the diagnostic criteria for ARDS, the following diseases were observed in patients without DAD, in order of descending

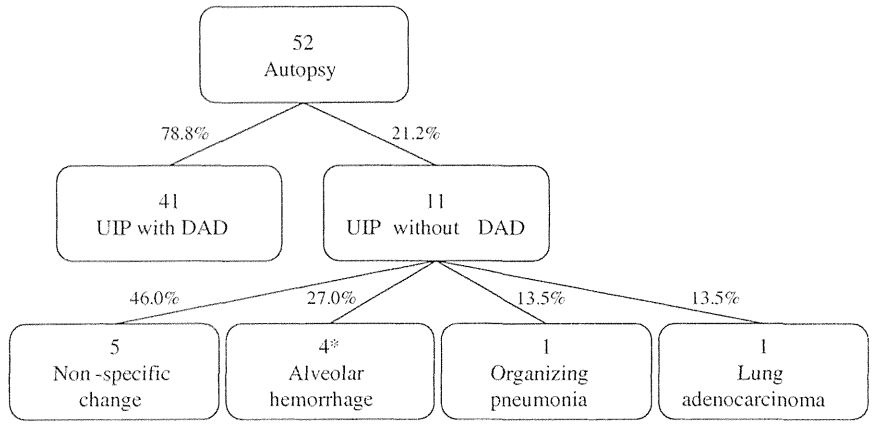

Figure 3 A flow diagram showing the pathological findings of the patients with AE-IPF. *One patient showed pulmonary thromboembolism with alveolar hemorrhage.

prevalence: pneumonia, pulmonary hemorrhage, pulmonary edema and pulmonary embolism [26]. The findings of such diverse pathological features are very similar to the results of the present study. To date, very few investigations have been carried out regarding the pathological findings of AE-IPF, and the present study is the first report to summarize the features of autopsy cases involving the "acute exacerbation" of IPF. In this study, although the diagnosis was made while checking the findings of AE-IPF against the diagnostic criteria, in the same manner as diagnosing ARDS, not all of the patients with AE-IPF exhibited DAD, namely only 78.8% of the AE-IPF patients demonstrated DAD. Moreover, a significant number of patients who satisfied the diagnostic criteria for AE-IPF did not have remarkable DAD (11/52, 21.2%). In addition, we found no findings associated with acute fibrinous or organizing pneumonia in the AE-IPF patients without DAD [27]. In these cases, genuine respiratory failure accompanied the progression of pulmonary fibrosis, which may constitute the natural course of IPF. Notably, the results of the present study are supported by the findings of a previous report in which only extensive fibroblastic foci were observed as a pathological finding of an acute pattern [13]. The incidence of gastrointestinal hemorrhage and right ventricular hypertrophy, both of which are extrapulmonary findings, was 25.0% and 34.6%, respectively.

Table 4 The characteristics of the 15 patients with positive results for infectious causes

Patient, No.	Age	Sex	Time from AE-IPF to death (days)	Prior treatment for IPF	Treatment for AE-IPF	Mechanical ventilation	Bacteria	Virus	Fungus
1	74	M	1	None	None	No	-	-	*Aspergillus* species
2	68	M	8	CS	High dose corticosteroids, CPA	Yes	-	CMV	-
3	66	M	10	None	High dose corticosteroids	Yes	-	-	*Aspergillus* species
4	67	M	12	None	High dose corticosteroids	Yes	GPC	-	-
5	76	F	13	CS	High dose corticosteroids, CPA	Yes	-	-	*Candia albicans*
6	78	M	15	None	High dose corticosteroids	No	GNR	CMV	-
7	68	M	19	None	High dose corticosteroids, CPA	Yes	GPC	-	-
8	83	M	19	CS, CsA	High dose corticosteroids, CsA	No	-	-	*Aspergillus* species
9	71	M	20	CS	High dose corticosteroids	Yes	-	-	*Aspergillus* species
10	68	M	22	None	High dose corticosteroids	Yes	-	CMV	-
11	81	M	35	CS	High dose corticosteroids, CPA	No	-	-	*Aspergillus* species
12	68	F	38	None	High dose corticosteroids, CPA	Yes	-	CMV	-
13	59	M	41	CS, CsA	High dose corticosteroids	No	GPC, GNR	CMV	-
14	76	M	58	None	High dose corticosteroids, CPA	Yes	-	CMV	-
15	80	M	122	CS	High dose corticosteroids	No	GNR	-	*Aspergillus* species

Abbreviations: AE-IPF Acute exacerbation of idiopathic pulmonary fibrosis, *CS* Corticosteroid, *CPA* Cyclophosphamide, *CsA* Cyclosporine, *GPC* Gram-positive cocci, *GNR* Gram-negative rods, *CMV* Cytomegalovirus.

Furthermore, the effects of hypoxic, physical and psychosomatic stress [28] and high-dose corticosteroid therapy [29] must be considered with respect to gastrointestinal hemorrhage. Right ventricular hypertrophy may be caused by pulmonary hypertension [30] at the end stage of AE-IPF. Moreover, the relationship between IPF and pulmonary hypertension is important, and Judge and colleagues recently reported that pulmonary hypertension is associated with acute disease exacerbation as well as poor survival [31]. Therefore, it is necessary to monitor the potential for pulmonary hypertension in patients with IPF.

Although there is no established standard therapy for AE-IPF [10], high-dose corticosteroid therapy [11,12,14,32-34] and immunosuppressive agents [35,36] are commonly used in clinical practice. However, a previous study [37] suggested that these drugs increase the rates of infectious complications. In addition to the immunodeficient state caused by corticosteroids and/or immunosuppressants, the application of intensive antimicrobial treatment following the acute exacerbation of pulmonary infection may have affected the results of the present study. Regardless, similar to recently published data [38] from a study of gene expression profiling of patients with AE-IPF, our data demonstrated that an infectious etiology may not be the main cause of AE-IPF. In fact, all patients underwent treatment with high-dose corticosteroids and/or immunosuppressive agents, excluding only one patient, with mechanical ventilation carried out in more than half of the AE-IPF patients. Moreover, the pulmonary infections detected in the present study may have affected, at least in part, the occurrence of respiratory failure leading to death, although there were no significant differences in the time interval between the diagnosis of AE-IPF and death based on the presence of infectious disease. Therefore, in addition to the detection of pathological findings based on DAD, AE-IPF eventually causes respiratory failure due to the effects of accompanying infectious diseases, with patients thus exhibiting a variety of histopathological features. The present investigation was carried out among autopsy cases only; therefore, the efficacy of high-dose corticosteroid therapy against AE-IPF cannot be debated based on our results. However, taking into consideration the fact that many patients with diabetes and pneumothorax following acute disease exacerbation underwent high-dose corticosteroid therapy, such therapy should be carefully administered based on the tolerability and efficacy of the treatment in conjunction with multidisciplinary therapies. Physicians should therefore be aware of the appropriate therapeutic strategies when treating patients with complications induced by treatment for AE-IPF. Furthermore, the results of the present study indicate that it is difficult to distinguish acute exacerbation from other disorders, even if the patient meets the diagnostic criteria for AE-IPF. Given the results of this study, it is very important for clinicians to be alert to the possibility of other treatable disorders, such as infectious diseases, as no effective treatment regimen for AE-IPF has been established to date.

There are several limitations associated with this study. First, only patients who died and underwent autopsy were included; therefore, the results may differ based on the status of onset of AE-IPF. In other words, no patients who survived after AE-IPF were included, and the present findings thus do not reflect all aspects of the entity of AE-IPF. Second, we did not perform endotracheal aspiration or bronchoalveolar lavage due to the presence of severe hypoxemia in all cases. However, we carefully excluded patients based on the findings of sputum, laboratory and physical examinations. In addition, a previous study reported that the features of clinically suspected acute exacerbation diagnosed based on the radiological and clinical course are similar to those of acute exacerbation diagnosed based on the results of several intensive examinations, including BAL [39]. Third, this study was carried out jointly across multiple facilities, primarily university hospitals, including only Japanese IPF patients. Hence, potential biases, including racial and institutional selection, must be considered when interpreting the results. Finally, 52% of the patients with AE-IPF in the present study required mechanical ventilation on admission, which suggests that these patients had a relatively more severe condition. Therefore, the results of this study may not be extrapolated to all cases of AE-IPF.

Conclusions

The pathological findings of AE-IPF include DAD as well as a variety of pathological conditions, and making a definitive diagnosis of AE-IPF is difficult. Patients with AE-IPF therefore are at risk of death due to the occurrence of several complications during their clinical course, including the effects of treatment with high-dose corticosteroid therapy. In patients with AE-IPF, it is very important to treat the disease by monitoring the patient's condition and timely intervening with appropriate treatment.

Abbreviations

IPF: Idiopathic pulmonary fibrosis; AE-IPF: Acute exacerbation of idiopathic pulmonary fibrosis; UIP: Usual interstitial pneumonia; DAD: Diffuse alveolar damage; OP: Organizing pneumonia; HRCT: High-resolution computed tomography; BAL: Bronchoalveolar lavage; H&E: Hematoxylin and eosin; PAS: Periodic acid-Schiff; CMV: Cytomegalovirus; RV: Right ventricular; LV: Left ventricular; ARDS: Acute respiratory distress syndrome.

Competing interests

The authors declare that they have no competing interests.

Authors' contributions

KO, HI and SY made substantial contributions to the conception and design of the study. KO, HK, HI, TI, TH, YI, NM and KN acquired the data. HI and KY analyzed and interpreted the data. KO, HI, MN, JK, KW, SK and HM participated

in drafting the article and critically revising it for important intellectual content. All authors have read and approved the final manuscript.

Acknowledgements

This research was partly supported by a grant to the Diffuse Lung Diseases Research Group from the Ministry of Health, Labour and Welfare, Japan and was a Ministry of Education, Science, Sports and Culture Grant-in-Aid for Scientific Research (B), 2013–2014 (25860665, Keishi Oda)

The authors thank all test personnel for their work during the data collection at the six institutions involved in the study: University of Occupational and Environmental Health, Japan, Oita University Faculty of Medicine, Fukuoka University School of Medicine, Steel Memorial Yawata Hospital, Nagasaki University School of Medicine and Miyazaki University School of Medicine. The authors also thank Drs. Chiharu Yoshii, Yukiko Kawanami, Toshinori Kawanami, Chinatsu Nishida, Kei Yamasaki, Shingo Noguchi, Takaaki Ogoshi, Kentarou Akata, Kaori Kato, Tetsuya Hanaka, and Masahiro Tahara for their cooperation in this research.

Author details

[1]Department of Respiratory Medicine, University of Occupational and Environmental Health, 1-1, Iseigaoka, Yahatanishiku, Kitakyushu City, Fukuoka 807-8555, Japan. [2]Department of Pathology and Cell Biology, University of Occupational and Environmental Health, 1-1, Iseigaoka, Yahatanishiku, Kitakyushu City, Fukuoka 807-8555, Japan. [3]Department of Respiratory Medicine and Infectious Diseases, Oita University Faculty of Medicine, 1-1 Idaigaoka, Hasama-machi, Oita 879-5593, Japan. [4]Department of Respiratory Medicine, Fukuoka University School of Medicine, 7-45-1, Nakakuma, Jonanku, Fukuoka 814-0180, Japan. [5]Department of Respiratory Medicine, Steel Memorial Yawata Hospital, 1-1-1, Harunomachi, Yahatahigashiku, Kitakyushu City, Fukuoka 805-8508, Japan. [6]Second Department of Internal Medicine, Nagasaki University School of Medicine, 1-7-1 Sakamoto, Nagasaki 852-8501, Japan. [7]Neurology, Respirology, Endocrinology and Metabolism, Internal Medicine, Faculty of Medicine, University of Miyazaki, 889-1692 Miyazaki, Japan.

Received: 14 July 2014 Accepted: 26 August 2014
Published: 1 September 2014

References

1. Bjoraker JA, Ryu JH, Edwin MK, Myers JL, Tazelaar HD, Schroeder DR, Offord KP: **Prognostic significance of histopathologic subsets in idiopathic pulmonary fibrosis.** *Am J Respir Crit Care Med* 1998, **157**:199–203.
2. Flaherty KR, Toews GB, Travis WD, Colby TV, Kazerooni EA, Gross BH, Jain A, Strawderman RL, Paine R, Flint A, Lynch JP, Martinez FJ: **Clinical significance of histological classification of idiopathic interstitial pneumonia.** *Eur Respir J* 2002, **19**:275–283.
3. Nicholson AG, Colby TV, du Bois RM, Hansell DM, Wells AU: **The prognostic significance of the histologic pattern of interstitial pneumonia in patients presenting with the clinical entity of cryptogenic fibrosing alveolitis.** *Am J Respir Crit Care Med* 2000, **162**:2213–2217.
4. Rudd RM, Prescott RJ, Chalmers JC, Johnston ID, Fibrosing Alveolitis Subcommittee of the Research Committee of the British Thoracic Society: **British Thoracic Society Study on cryptogenic fibrosing alveolitis: Response to treatment and survival.** *Thorax* 2007, **62**:62–66.
5. Kondoh Y, Taniguchi H, Katsuta T, Kataoka K, Kimura T, Nishiyama O, Sakamoto K, Johkoh T, Nishimura M, Ono K, Kitaichi M: **Risk factors of acute exacerbation of idiopathic pulmonary fibrosis.** *Sarcoidosis Vasc Diffuse Lung Dis* 2010, **27**:103–110.
6. Ley B, Collard HR, King TE: **Clinical course and prediction of survival in idiopathic pulmonary fibrosis.** *Am J Respir Crit Care Med* 2011, **183**:431–440.
7. Kondoh Y, Taniguchi H, Kawabata Y, Yokoi T, Suzuki K, Takagi K: **Acute exacerbation in idiopathic pulmonary fibrosis. Analysis of clinical and pathologic findings in three cases.** *Chest* 1993, **103**:1808–1812.
8. Society AT, Society ER: **American Thoracic Society/European Respiratory Society International Multidisciplinary Consensus Classification of the Idiopathic Interstitial Pneumonias. This joint statement of the American Thoracic Society (ATS), and the European Respiratory Society (ERS) was adopted by the ATS board of directors, June 2001 and by the ERS Executive Committee, June 2001.** *Am J Respir Crit Care Med* 2002, **165**:277–304.
9. Collard HR, Moore BB, Flaherty KR, Brown KK, Kaner RJ, King TE, Lasky JA, Loyd JE, Noth I, Olman MA, Raghu G, Roman J, Ryu JH, Zisman DA, Hunninghake GW, Colby TV, Egan JJ, Hansell DM, Johkoh T, Kaminski N, Kim DS, Kondoh Y, Lynch DA, Müller-Quernheim J, Myers JL, Nicholson AG, Selman M, Toews GB, Wells AU, Martinez FJ: **Acute exacerbations of idiopathic pulmonary fibrosis.** *Am J Respir Crit Care Med* 2007, **176**:636–643.
10. Raghu G, Collard HR, Egan JJ, Martinez FJ, Behr J, Brown KK, Colby TV, Cordier JF, Flaherty KR, Lasky JA, Lynch DA, Ryu JH, Swigris JJ, Wells AU, Ancochea J, Bouros D, Carvalho C, Costabel U, Ebina M, Hansell DM, Johkoh T, Kim DS, King TE Jr, Kondoh Y, Myers J, Müller NL, Nicholson AG, Richeldi L, Selman M, Dudden RF, *et al*: **An official ATS/ERS/JRS/ALAT statement: idiopathic pulmonary fibrosis: evidence-based guidelines for diagnosis and management.** *Am J Respir Crit Care Med* 2011, **183**:788–824.
11. Kim DS, Park JH, Park BK, Lee JS, Nicholson AG, Colby T: **Acute exacerbation of idiopathic pulmonary fibrosis: frequency and clinical features.** *Eur Respir J* 2006, **27**:143–150.
12. Ambrosini V, Cancellieri A, Chilosi M, Zompatori M, Trisolini R, Saragoni L, Poletti V: **Acute exacerbation of idiopathic pulmonary fibrosis: report of a series.** *Eur Respir J* 2003, **22**:821–826.
13. Churg A, Muller NL, Silva CI, Wright JL: **Acute exacerbation (acute lung injury of unknown cause) in UIP and other forms of fibrotic interstitial pneumonias.** *Am J Surg Pathol* 2007, **31**:277–284.
14. Parambil JG, Myers JL, Ryu JH: **Histopathologic features and outcome of patients with acute exacerbation of idiopathic pulmonary fibrosis undergoing surgical lung biopsy.** *Chest* 2005, **128**:3310–3315.
15. Katzenstein AL, Bloor CM, Leibow AA: **Diffuse alveolar damage–the role of oxygen, shock, and related factors. A review.** *Am J Pathol* 1976, **85**:209–228.
16. Sulavik SB: **The concept of "organizing pneumonia".** *Chest* 1989, **96**:967–969.
17. Forman MB, Wilson BH, Sheller JR, Kopelman HA, Vaughn WK, Virmani R, Friesinger GC: **Right ventricular hypertrophy is an important determinant of right ventricular infarction complicating acute inferior left ventricular infarction.** *J Am Coll Cardiol* 1987, **10**:1180–1187.
18. Nadrous HF, Pellikka PA, Krowka MJ, Swanson KL, Chaowalit N, Decker PA, Ryu JH: **Pulmonary hypertension in patients with idiopathic pulmonary fibrosis.** *Chest* 2005, **128**:2393–2399.
19. Sawabe M, Saito M, Naka M, Kasahara I, Saito Y, Arai T, Hamamatsu A, Shirasawa T: **Standard organ weights among elderly Japanese who died in hospital, including 50 centenarians.** *Pathol Int* 2006, **56**:315–323.
20. Husari A, Beydoun A, Sheik Ammar A, Maakaron JE, Taher A: **The untold story of Dabigatran etexilate: alveolar hemorrhage in an elderly patient with interstitial pulmonary fibrosis.** *J Thromb Thrombolysis* 2013, **35**:81–82.
21. Perri D, Cole DE, Friedman O, Piliotis E, Mintz S, Adhikari NK: **Azathioprine and diffuse alveolar haemorrhage: the pharmacogenetics of thiopurine methyltransferase.** *Eur Respir J* 2007, **30**:1014–1017.
22. Birnbaum J, Danoff S, Askin FB, Stone JH: **Microscopic polyangiitis presenting as a "pulmonary-muscle" syndrome: is subclinical alveolar hemorrhage the mechanism of pulmonary fibrosis?** *Arthritis Rheum* 2007, **56**:2065–2071.
23. Sakamoto K, Taniguchi H, Kondoh Y, Wakai K, Kimura T, Kataoka K, Hashimoto N, Nishiyama O, Hasegawa Y: **Acute exacerbation of IPF following diagnostic bronchoalveolar lavage procedures.** *Respir Med* 2012, **106**:436–442.
24. Sprunger DB, Olson AL, Huie TJ, Fernandez-Perez ER, Fischer A, Solomon JJ, Brown KK, Swigris JJ: **Pulmonary fibrosis is associated with an elevated risk of thromboembolic disease.** *Eur Respir J* 2012, **39**:125–132.
25. Patel SR, Karmpaliotis D, Ayas NT, Mark EJ, Wain J, Thompson BT, Malhotra A: **The role of open-lung biopsy in ARDS.** *Chest* 2004, **125**:197–202.
26. Esteban A, Fernández-Segoviano P, Frutos-Vivar F, Aramburu JA, Nájera L, Ferguson ND, Alía I, Gordo F, Rios F: **Comparison of clinical criteria for the acute respiratory distress syndrome with autopsy findings.** *Ann Intern Med* 2004, **141**:440–445.
27. Beasley MB, Franks TJ, Galvin JR, Gochuico B, Travis WD: **Acute fibrinous and organizing pneumonia: a histological pattern of lung injury and possible variant of diffuse alveolar damage.** *Arch Pathol Lab Med* 2002, **126**:1064–1070.
28. Cook DJ, Fuller HD, Guyatt GH, Marshall JC, Leasa D, Hall R, Winton TL, Rutledge F, Todd TJ, Roy P: **Risk factors for gastrointestinal bleeding in critically ill patients. Canadian Critical Care Trials Group.** *N Engl J Med* 1994, **330**:377–381.
29. Hernández-Díaz S, Rodríguez LA: **Steroids and risk of upper gastrointestinal complications.** *Am J Epidemiol* 2001, **153**:1089–1093.
30. Lettieri CJ, Nathan SD, Barnett SD, Ahmad S, Shorr AF: **Prevalence and outcomes of pulmonary arterial hypertension in advanced idiopathic pulmonary fibrosis.** *Chest* 2006, **129**:746–752.
31. Judge EP, Fabre A, Adamali HI, Egan JJ: **Acute exacerbations and pulmonary hypertension in advanced idiopathic pulmonary fibrosis.** *Eur Respir J* 2012, **40**:93–100.

32. Azuma A, Nukiwa T, Tsuboi E, Suga M, Abe S, Nakata K, Taguchi Y, Nagai S, Itoh H, Ohi M, Sato A, Kudoh S: **Double-blind, placebo-controlled trial of pirfenidone in patients with idiopathic pulmonary fibrosis.** *Am J Respir Crit Care Med* 2005, **171**:1040–1047.
33 Kubo H, Nakayama K, Yanai M, Suzuki T, Yamaya M, Watanabe M, Sasaki H: **Anticoagulant therapy for idiopathic pulmonary fibrosis.** *Chest* 2005, **128**:1475–1482.
34. Kim DS, Collard HR, King TE: **Classification and natural history of the idiopathic interstitial pneumonias.** *Proc Am Thorac Soc* 2006, **3**:285–292.
35. Inase N, Sawada M, Ohtani Y, Miyake S, Isogai S, Sakashita H, Miyazaki Y, Yoshizawa Y: **Cyclosporin A followed by the treatment of acute exacerbation of idiopathic pulmonary fibrosis with corticosteroid.** *Intern Med* 2003, **42**:565–570.
36. Sakamoto S, Homma S, Miyamoto A, Kurosaki A, Fujii T, Yoshimura K: **Cyclosporin A in the treatment of acute exacerbation of idiopathic pulmonary fibrosis.** *Intern Med* 2010, **49**:109–115.
37. Stuck AE, Minder CE, Frey FJ: **Risk of infectious complications in patients taking glucocorticosteroids.** *Rev Infect Dis* 1989, **11**:954–963.
38. Konishi K, Gibson KF, Lindell KO, Richards TJ, Zhang Y, Dhir R, Bisceglia M, Gilbert S, Yousem SA, Song JW, Kim DS, Kaminski N: **Gene expression profiles of acute exacerbations of idiopathic pulmonary fibrosis.** *Am J Respir Crit Care Med* 2009, **180**:167–175.
39. Collard HR, Yow E, Richeldi L, Anstrom KJ, Glazer C, IPFnet investigators: **Suspected acute exacerbation of idiopathic pulmonary fibrosis as an outcome measure in clinical trials.** *Respir Res* 2013, **14**:73.

doi:10.1186/s12931-014-0109-y
Cite this article as: Oda *et al.*: Autopsy analyses in acute exacerbation of idiopathic pulmonary fibrosis. *Respiratory Research* 2014 **15**:109.

NUTRITION RESEARCH 34 (2014) 876–885

Available online at www.sciencedirect.com

ScienceDirect

www.nrjournal.com

Rikkunshito ameliorates cachexia associated with bleomycin-induced lung fibrosis in mice by stimulating ghrelin secretion

Hironobu Tsubouchi[a], *Shigehisa Yanagi*[a], *Ayako Miura*[a], *Sachiko Mogami*[b], *Chihiro Yamada*[b], *Seiichi Iizuka*[b], *Tomohisa Hattori*[b], *Masamitsu Nakazato*[a,*]

[a] *Division of Neurology, Respirology, Endocrinology and Metabolism, Department of Internal Medicine, Faculty of Medicine, University of Miyazaki, Kiyotake, Miyazaki 889-1692, Japan*

[b] *Tsumura Research Laboratories, Tsumura and Co, 3586 Yoshiwara, Ami-machi, Inashiki-gun, Ibaraki 300-1192, Japan*

ARTICLE INFO

Article history:
Received 2 May 2014
Revised 30 July 2014
Accepted 27 August 2014

Keywords:
Rikkunshito
Cachexia
Ghrelin
Lung fibrosis
Bleomycin
Mice

ABSTRACT

Cachexia is a frequent complication in patients with respiratory failure, such as lung fibrosis, and it is a determining factor for functional capacity, health status, and mortality. Reductions in body weight and skeletal muscle mass are key features of cachexia that are resistant to current therapies. Rikkunshito (RKT), a traditional Japanese herbal medicine, is widely used for the treatment for patients with gastrointestinal symptoms and known to stimulate ghrelin secretion. By using bleomycin (BLM)-induced lung fibrosis mice in this study, we tested our hypothesis that RKT administration could ameliorate pulmonary cachexia. After BLM administration, mice were provided with either RKT or distilled water on a daily basis. Compared with the BLM-injected mice, the RKT-treated mice had smaller reductions of food intake and body weight. Skeletal muscle weights were retained in the RKT-treated mice, in conjunction with reduced expressions of MuRF-1 and atrogin-1 in the lysates of skeletal muscle found in lung fibrosis. Rikkunshito administration restored the plasma concentrations of ghrelin in BLM-injected mice. The anticachectic efficacies of RKT administration in BLM-injected mice were canceled by the concurrent treatment of a ghrelin receptor antagonist. Rikkunshito administration did not decrease the degree of loss of body weight or food intake reduction in either ghrelin-deficient mice or growth hormone secretagogue receptor–deficient mice. Our results indicate that RKT administration exerts protective effects on pulmonary cachexia by ameliorating skeletal muscle wasting and food intake reduction as mediated by the ghrelin system and, thus, highlight RKT as a potential therapeutic agent for the management of lung fibrosis.

1. Introduction

Cachexia is a critical illness that consists of skeletal muscle wasting and reduction in body weight [1]. Chronic disorders are complicated by cachexia, including cancer [1] and chronic respiratory failure [2]. Patients with terminal-stage chronic respiratory disease, such as chronic obstructive pulmonary disease (COPD) and interstitial lung disease, have common

Abbreviations: BLM, bleomycin; RKT, rikkunshito; GAPDH, glyceraldehyde 3-phosphate dehydrogenase; DW, distilled water; 5HT2B receptor, serotonin 2B receptor; *Ghsr*$^{-/-}$, growth hormone secretagogue receptor–deficient; *ghrelin*$^{-/-}$, ghrelin-deficient.

* *Corresponding author.* Division of Neurology, Respirology, Endocrinology and Metabolism, Department of Internal Medicine, Faculty of Medicine, University of Miyazaki, Kiyotake, Miyazaki 889-1692, Japan. Tel.: +81 985 85 2965; fax: +81 985 85 1869.
E-mail address: nakazato@med.miyazaki-u.ac.jp (M. Nakazato).

http://dx.doi.org/10.1016/j.nutres.2014.08.014
0271-5317/

clinical features. These clinical features include the development of dyspnea [3,4], an increase in resting energy expenditure [5,6], and skeletal muscle weakness [2], and all of these can lead to further deterioration of respiratory function. Several studies demonstrated that reductions of muscle mass [7] and body weight [8,9] are important prognostic factors in patients who have chronic respiratory failure caused by COPD or interstitial lung disease. Thus, the development of therapeutic strategies for cachectic conditions, including retention of body weight, food intake, and/or muscle mass, may provide protective effects in patients with these respiratory diseases.

Ghrelin is a 28-amino-acid peptide that was initially isolated from human and rat stomach as an endogenous ligand of growth hormone secretagogue receptor [10]. In addition to its stimulatory action on growth hormone release [10], ghrelin is known to have multifaceted effects on energy metabolism, which includes the promotion of food intake [11] and the prevention of muscle catabolism [12]. A previous study reported the effectiveness of ghrelin in the treatment of the skeletal muscle wasting that is associated with COPD [13]. Rikkunshito (RKT) is a Kampo (traditional Japanese herbal) medicine that is used in Japan to treat various gastrointestinal tract disorders, such as decrease gastric motility after surgery [14] and functional dyspepsia [15]. Rikkunshito stimulated the secretion of ghrelin and its downstream signals in humans [15], and RKT improved anorexia in tumor-bearing rats [16]. We recently reported that both ghrelin [17] and RKT [18] administrations mitigated lung inflammation and fibrosis in a bleomycin (BLM)-induced acute lung injury model in mice. However, the effects of RKT treatment on muscle wasting and its precise mechanisms in conditions involving respiratory failure (including lung fibrosis) are not known. Because RKT promotes ghrelin secretion, we hypothesized that RKT would have a protective effect against the cachexia associated with lung fibrosis via ghrelin secretion. The objective of the present study was to investigate the efficacy of RKT administration in the amelioration of cachexia in a BLM-induced lung fibrosis model in mice. We also investigated whether RKT administration mitigates the cachexia associated with lung fibrosis dependently or independently of the ghrelin system.

2. Methods and materials

2.1. Animals

Ten-week-old male C57BL/6J mice (wild-type [WT] mice) were purchased from Charles River Japan (Yokohama, Japan). Ten-week-old ghrelin-deficient (*ghrelin*$^{-/-}$) C57/B6/6N mice [19] were generously provided by Dr Masayasu Kojima (Kurume University). Growth hormone secretagogue receptor–deficient (*Ghsr*$^{-/-}$) C57/B6/6N mice [20] were generously provided by Dr. Roy G. Smith (Baylor College of Medicine, Houston, TX, USA). All mice weighed 22 to 29 g and were individually housed in plastic cages. They were kept in an air-conditioned room with the temperature set at 23 ± 1°C, humidity fixed at 55% ± 10%, and with a 12-hour light/dark cycle. The mice were fed a standard laboratory chow with ad libitum access to food, unless otherwise stated in the study protocol. All experimental procedures were performed in accordance with the Japanese Physiological Society's Guidelines for Animal Care and approved by the Ethics Committee on Animal Experimentation of the University of Miyazaki and the Laboratory Animal Committee of Tsumura & Co (Ibaraki, Tokyo).

2.2. Chemicals

Bleomycin, ghrelin receptor antagonist ([D-Lys^3]-GHRP-6), and serotonin 2B (5HT2B) receptor antagonist (SB215505) were obtained from Sigma-Aldrich (St Louis, MO, USA) and dissolved in sterilized saline. Rikkunshito (Tsumura & Co) was industrially made from a hot water extract that included a mixture of 8 types of the following medical herbs: *Atractylodes lancea* rhizome (4.0 g), *Ginseng radix* (4.0 g), *Pinelliae tuber* (4.0 g), *Hoelen* (4.0 g), *Zizyphi fructus* (2.0 g), *Aurantii nobilis pericarpium* (2.0 g), *Glycyrrhizae radix* (1.0 g), and *Zingiberis rhizome* (0.5 g). It was then spray-dried, and RKT was dissolved in distilled water (DW).

2.3. Bleomycin administration

The intratracheal administration of BLM was performed, as previously described [21]. Briefly, mice were anesthetized by an intraperitoneal administration of pentobarbital sodium and were intratracheally administered 3.0 mg/kg of BLM that was dissolved in either 50 μL sterile saline or 50 μL sterile saline.

2.4. RKT administration for the determination of its effects on lung fibrosis, food intake, body weight, and muscle wasting in BLM-injected mice

At 3 days prior to the above-described BLM administration, either RKT (1000 mg/kg) or DW was orally administered by gavage. We designated the BLM-injected, RKT-treated mice as the BLM/RKT group; the BLM-injected, DW-treated mice as the BLM/DW group; and the saline-injected, DW-treated mice as the saline/DW group. Starting with 1 day before and continuing until the 10th day of the BLM or saline instillation, body weights and food intake were measured daily. We used the BLM/RKT, BLM/DW, and saline/DW groups for the measurements of body weights and food intake (n = 7-11 per group of WT mice, n = 6-13 per group of *ghrelin*$^{-/-}$ mice, and n = 7-8 per group of *Ghsr*$^{-/-}$ mice). For the histologic assay (n = 5 per group of WT mice), the immunohistochemical analyses (n = 5 per group of WT mice), the measurements of the mean cross-sectional area of the gastrocnemius muscle (n = 5 per group of WT mice), the measurements of the weight of the gastrocnemius muscle (n = 7-8 per group of WT mice), the Sircol collagen assay (n = 7-8 per group of WT mice), and the quantitative reverse transcription polymerase chain reaction (qRT-PCR; n = 7-8 per group of WT mice), we used 3 additional groups and examined the animals on day 14. In the analyses of lung fibrosis, food intake, body weight, and muscle wasting, we used the saline/DW group as the control group.

2.5. The administration of RKT for the determination of its effects on ghrelin secretion in BLM-injected mice

To evaluate the effect of RKT administration on ghrelin secretion, we used the saline/DW group (control group), the BLM/DW group (n = 10), the BLM/RKT pair-fed group (n = 10), and the saline/DW pair-fed group (n = 10). We collected blood samples from the mice

of these groups on the fifth day. The BLM/RKT pair-fed group and the saline/DW pair-fed group were fed the same quantities of diet, as consumed by the mice in the BLM/DW group [22]. Briefly, the BLM/DW group was administered BLM 1 day before the saline injection was given to the saline/DW pair-fed group and the BLM injection was given to the BLM/RKT pair-fed group, and the amount of food intake was measured. The saline/DW pair-fed group and the BLM/RKT pair-fed group were given access to the same amount of food that was consumed by the BLM/DW group on the previous day.

2.6. *The administration of growth hormone secretagogue receptor antagonist for the evaluation of its effect on food intake in the BLM-injected, RKT-treated mice*

At 3 days before the BLM administration, either RKT (1000 mg/kg) or DW was orally administered by gavage. Starting 1 day after the BLM injection, either [D-Lys^3]-GHRP-6 (5 or 10 μmol/kg) dissolved in saline or saline alone was intraperitoneally administered daily during the 7-day interval. We designated the BLM-injected, RKT-treated, [D-Lys^3]-GHRP-6-treated mice as the BLM/RKT/[D-Lys^3]-GHRP-6 group; the BLM-injected, RKT-treated, saline-treated mice as the BLM/RKT/saline group; the BLM-injected, DW-treated, saline-treated mice as the BLM/DW/saline group; and the saline-injected, DW-treated, saline-treated mice as the saline/DW/saline group (ie, control group). The food intake was measured daily from 1 day before the BLM or saline administration until the seventh day. For the measurements of food intake in WT, we used the BLM/RKT/[D-Lys^3]-GHRP-6 (5 μmol/kg; n = 19), BLM/RKT/[D-Lys^3]-GHRP-6 (10 μmol/kg; n = 16), the BLM/RKT/saline (n = 13), the BLM/DW/saline (n = 16), and the saline/DW/saline (n = 19) groups.

2.7. *The administration of 5HT2B receptor antagonist for the evaluation of its effects on food intake and ghrelin secretion in BLM-injected mice*

Starting 1 day after the BLM injection, either SB215505 (6.0 mg/kg) dissolved in saline or saline alone was intraperitoneally administered daily, during the 5-day interval. We designated the saline-injected, saline-treated mice as the saline/saline group (control group); the BLM-injected, saline-treated mice as the BLM/saline group; and the BLM-injected, SB215505-treated mice as the BLM/SB215505 group. For the evaluation of the short-term effects of SB215505 on food intake, we measured the 6-hour food intake amounts on day 5 of the SB215505 and saline treatment groups. For the measurements of food intake, we used the saline/saline (n = 10), BLM/saline (n = 10), and BLM/SB215505 (n = 10) groups. To evaluate the effect of 5HT2B receptor antagonist on ghrelin secretion, on the fifth day we examined the following groups: saline/saline (control; n = 10), the saline/saline pair-fed (n = 10), the BLM/saline (n = 10), and the BLM/SB215505 pair-fed (n = 10). The saline/saline pair-fed group and the BLM/SB215505 pair-fed group were fed the same quantities of diet as consumed by the animals of the BLM/saline group.

2.8. *Measurement of plasma ghrelin levels*

Five days after either BLM or saline injection, blood was taken by heart puncture and collected in a tube containing aprotinin and ethylenediaminetetraacetic acid (Wako, Osaka, Japan). It was mixed well and immediately centrifuged at 4°C. After plasma collection, a 1/10 volume of 1 mol/L HCl was added. The prepared plasma was stored at −80°C until the measurement of ghrelin. Ghrelin levels were determined using an Active Ghrelin or Desacyl-Ghrelin ELISA Kit (Mitsubishi Kagaku Iatron, Tokyo, Japan), as previously described [23].

2.9. *Histology of the lungs*

The lungs were removed 14 days after the saline or BLM injection, fixed in 10% buffered formalin solution, and embedded in Optimal cutting temperature compound (Sakura Finetek, Tokyo, Japan). Lung sections (4 μm thick) were mounted on slides and stained with hematoxylin-eosin, as previously described [18].

2.10. *Measurement of lung collagen levels*

The collagen contents in the lungs were measured by the Sircol collagen assay, as previously described [17]. Briefly, the lungs were removed 14 days after BLM or saline injection, washed with cold phosphate-buffered saline, frozen in liquid nitrogen, and stored at −70°C until use. The lungs were homogenized in 1 mL of 0.5 M acetic acid solution by a TissueLyser II (Qiagen, Hilden, Germany). The homogenate samples were mixed with 4 mL of 0.5 M acetic acid solution and pepsin (0.1 mg/mL), incubated overnight at 4°C, and centrifuged at 13 000×*g* for 10 minutes. Total lung collagen levels were determined by measuring soluble collagen in the lungs with a Sircol collagen assay kit (Biocolor, Carrickfergus, UK), according to the instructions of the manufacturer.

2.11. *Morphometry of muscle fibers*

The gastrocnemius muscles were removed and weighed 14 days after BLM or saline treatment, fixed in 10% buffered formalin solution, and embedded in Optimal cutting temperature compound. The cross-sectional areas of the gastrocnemius muscle were measured, as previously described [24]. Briefly, the muscle sections (6 μm) were mounted on slides for immunostaining with an antibody recognizing laminin (Sigma-Aldrich, Tokyo, Japan). For each muscle section, the whole muscle cross section was analyzed to calculate the average fiber size (cross-sectional area) by using Image J 1.46 (freeware developed by Dr W. Rasband at the Research Services Branch, US National Institute of Mental Health, and available at http://rsb.info.nih.gov/ij). The cross-sectional areas of muscle sections from 5 mice per group were quantified by using the Image J. The mean of the cross-sectional area was calculated based on the measurements of 166-296 myofibers per mouse.

2.12. *Extraction of messenger RNA and qRT-PCR*

As previously described, 14 days after BLM or saline treatment, we measured the messenger RNA (mRNA) levels of *atrogin-1* and *MuRF-1*[25]. Briefly, the mRNA was extracted from the whole gastrocnemius muscle using a Ribopure TM Kit (Life Technologies, Tokyo, Japan). First-strand cDNA was generated by reverse transcription, using a High Capacity RNA-to-cDNA Kit (Life Technologies). We conducted a qRT-PCR using Taqman Fast Universal PCR Master Mix (Life Technologies) and a Thermal Cycler Dice Real Time System II

(Takara Bio, Tokyo, Japan). The levels of mRNA were determined by using cataloged primers (Applied Biosystems, Foster City, CA, USA) for mice (atrogin-1: Mm00499523_m1 and *MuRF-1*: Mm01185221_m1). The expressions of these genes were normalized to the expression of glyceraldehyde-3-phosphate dehydrogenase (GAPDH) mRNA (glyceraldehyde-3-phosphate dehydrogenase: Mm99999915_g1), and the results are expressed as relative fold differences.

2.13. *Statistical analyses*

All values are expressed as the means ± SEM. Power analyses were performed to determine the required sample sizes for each group, based on the results of preliminary experiments for the measurements of the mRNA levels of *atrogin-1* in gastrocnemius muscles (saline/DW group: n = 8, BLM/DW group: n = 7, BLM/RKT group: n = 8, effect size: f = 0.78) by using G* Power 3 [26]. Assuming the statistical power was 0.8 and 0.9, the required sample sizes were estimated to be 7 animals per group and 9 animals per group, respectively, and the type I error probability was 0.05. Thus, we determined the sample sizes as approximately 7 to 10 mice per group. All values were analyzed using a 1-way analysis of variance (ANOVA) and followed by Dunnett multiple comparison test, by using JMP 10 (SAS Institute, Tokyo, Japan). Differences were considered significant at P values less than .05.

3. Results

3.1. *Rikkunshito administration reduced lung fibrosis in BLM-injected mice*

The lung sections from BLM/DW mice showed extensive lung fibrosis associated with the destruction of normal lung architecture (Fig. 1A, middle panel). Rikkunshito administration to the BLM-injected mice ameliorated lung fibrosis and, comparatively, preserved lung architecture (Fig. 1A, right panel). The Sircol collagen assay revealed a significant reduction of collagen contents in the BLM/RKT lungs (Fig. 1B).

3.2. *Rikkunshito administration attenuated weight loss and suppression of food intake in BLM-injected mice*

The BLM/DW group showed a significant reduction of body weight and food intake compared with the saline/DW control group (Fig. 2). Rikkunshito administration significantly attenuated weight loss and the decrease in food intake in the BLM-injected mice (Fig. 2).

3.3. *Rikkunshito administration decreased skeletal muscle wasting and the levels of catabolic factors in BLM-injected mice*

The gastrocnemius muscles of BLM/DW mice exhibited excessive shrinkage of muscle fibers and reduction of muscle weights, compared with the saline/DW muscles (Fig. 3A, B). Rikkunshito administration suppressed the reduction of muscle fiber size and the loss of muscle weights in the BLM-injected mice. The mRNA levels of *atrogin-1* and *MuRF-1* in the gastrocnemius muscles of the BLM/DW mice were significantly higher than those of the saline/DW mice (Fig. 3C). Rikkunshito administration decreased these parameters in the BLM-injected mice.

3.4. *Rikkunshito administration elevated the plasma levels of ghrelin and des-acyl ghrelin in the BLM-injected mice*

To evaluate the effect of RKT administration on ghrelin secretion, we used the saline/DW control, the saline/DW pair-fed, the BLM/DW, and the BLM/RKT pair-fed groups. The

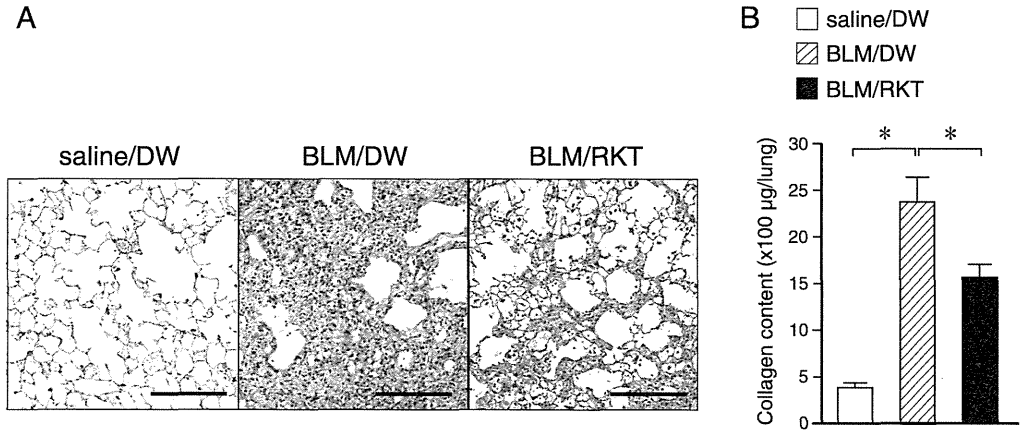

Fig. 1 – Effect of RKT administration on lung fibrosis in BLM-injected mice. A, Representative hematoxylin-eosin staining of 4-μm-thick lung sections of the saline/DW group, BLM/DW group, and BLM/RKT group after an injection of saline or 3.0 mg/kg of BLM on day 14. The saline/DW group is shown as the control group. The data are representative lung sections from 5 mice per group. Scale bars: 100 μm. B, Collagen contents in the lungs of saline/DW (425.4 ± 36.9 μg, n = 7), BLM/DW (2178.1 ± 220.4 μg, n = 7), and BLM/RKT mice (1560.8 ± 134.9 μg, n = 8) 14 days after an injection of saline or 3 mg/kg of BLM. Values are means ± SEM. Data were analyzed by an ANOVA, followed by Dunnett multiple comparison test. *P < .05.

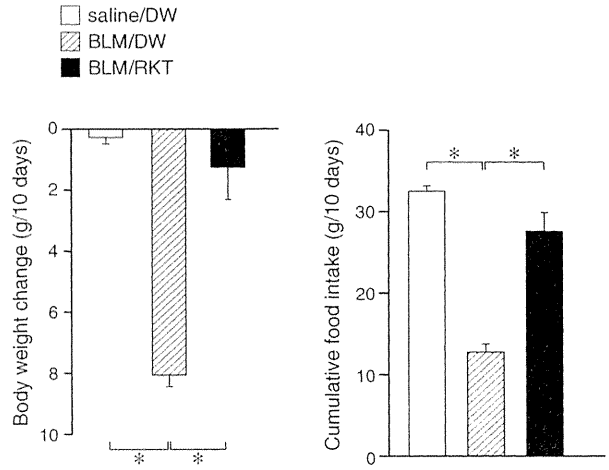

Fig. 2 – Effects of RKT administration on food intake and weight change in BLM-injected mice. Alterations in body weight (left) and cumulative food intake (right) 10 days after the instillation of 3.0 mg/kg of BLM or saline in WT mice. Respective body weight change and cumulative food intake values: saline/DW: −0.3 ± 0.2 g, 32.5 ± 0.6 g, n = 11; BLM/DW: −8.2 ± 0.3 g, 12.4 ± 1.2 g, n = 11; BLM/RKT: −1.2 ± 0.2 g, 27.7 ± 2.3 g, n = 7. Control group: saline/DW. Values are means ± SEM, analyzed by 1-way ANOVA and then Dunnett multiple comparison test. *P < .05.

plasma levels of ghrelin and des-acyl ghrelin in the BLM/DW mice were significantly lower than those of the saline/DW pair-fed mice (Fig. 4). In contrast, these parameters in the BLM/RKT pair-fed group were significantly higher than those of the BLM/DW group (Fig. 4).

3.5. *Rikkunshito administration mitigated the weight loss and reduction of food intake in BLM-injected mice, dependently of the ghrelin system*

The administration of RKT did not attenuate the degree of loss of body weight or food intake reduction in either the *ghrelin*$^{-/-}$ or *Ghsr*$^{-/-}$ mice, after BLM injection (Fig. 5A, B). The treatments with both 5 and 10 μmol/kg of [D-Lys^3]-GHRP-6 abrogated the ameliorative effect of RKT administration on the reduction of food intake in BLM-injected mice (Fig. 6).

3.6. *Serotonin 2B receptor antagonist administration mitigated the reduction of food intake and elevated the plasma levels of ghrelin and des-acyl ghrelin in BLM-injected mice*

We examined the mechanisms of how RKT stimulates ghrelin secretion in BLM-injected mice. Flavonoids contained in RKT, such as hesperetin, heptamethoxyflavone, and isoliquiritigenin, have 5HT2B receptor antagonistic activity [23]. It was reported that the administration of 5HT2B receptor antagonist attenuated the decreases in food intake and plasma ghrelin levels in cisplatin-treated rats [23]. Thus, we evaluated the influence of the antagonism of 5HT2B receptor on food intake and ghrelin secretion in BLM-injected mice. The administration of SB215505 mitigated the food intake reduction in BLM-injected mice (Fig. 7A). The levels of plasma ghrelin and des-acyl ghrelin in the BLM/SB215505 pair-fed group were higher than those of the BLM/saline group (Fig. 7B).

4. Discussion

The results of the present experiments demonstrate the protective effect of RKT against cachectic conditions associated with lung fibrosis. Rikkunshito administration mitigated the reduction of food intake, lessened body weight loss, and elevated plasma levels of ghrelin in BLM-injected mice. For the first time, we also demonstrated that RKT administration results in retained skeletal muscle mass in BLM-injected mice with a suppression of the expressions of the muscle-specific E3 ubiquitin ligases. Chronic respiratory diseases [9,27] such as lung fibrosis [28] lead to impaired function of skeletal muscles due to muscle wasting. This is a life-threatening condition [7,29] due to the impairment of normal activity and further deterioration of respiratory function. Prevention of skeletal muscle wasting is one of the top necessities for control of cachectic status associated with chronic respiratory disease [30]. However, current therapeutic strategies to combat muscle atrophy are quite limited. Our findings suggest that RKT may be developed into an effective treatment for pulmonary cachexia patients by exerting protective effects against decreased appetite and muscle wasting.

Rikkunshito significantly improved decreased food intake and body weight in mice with BLM-induced lung fibrosis, whereas administration of a ghrelin receptor antagonist reduced the food intake and body weight gain in obese mice [31]. In the present study, the plasma ghrelin levels in the BLM/DW mice were significantly lower than their counterparts in the saline/DW pair-fed mice group. Rikkunshito administration significantly elevated this parameter under the pair-fed condition in BLM-injected mice. The administration of the ghrelin receptor antagonist in BLM/RKT mice inhibited the RKT's alleviative effect on the reduction of food intake in BLM-injected mice. Moreover, the administration of

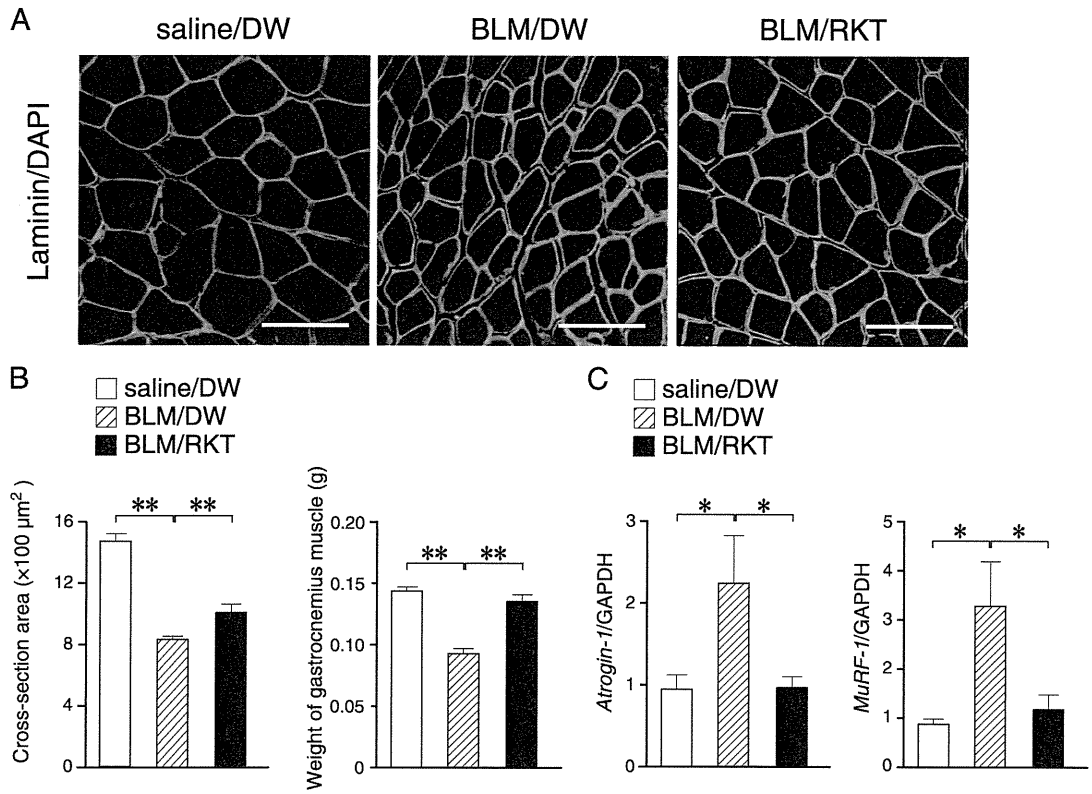

Fig. 3 – Effect of RKT administration on muscle wasting in BLM-injected mice. A, Representative profiles of immunostaining of laminin (green) of the 6-μm-thick sections of gastrocnemius muscles of the DW, BLM/DW, and BLM/RKT groups 14 days after BLM or saline treatment. Control group: saline/DW. Data shown are representative right gastrocnemius muscles sections (CSAs) from 5 mice per group. Scale bars: 200 μm. B, The mean cross-sectional areas of gastrocnemius myofibers are shown (saline/DW: 1481.7 ± 50.4 μm², BLM/DW: 835.3 ± 16.7 μm², BLM/RKT: 1011.9 ± 59.4 μm²). The mean CSA of the right gastrocnemius muscle was calculated based on the measurements of 166 to 296 myofibers per muscle from 5 mice per group, by using Image J 1.46. Values are means ± SEM. C, The mean weights of gastrocnemius muscles (saline/DW: 0.153 ± 0.004 g, n = 8; BLM/DW: 0.104 ± 0.005, n = 7; BLM/RKT: 0.124 ± 0.007, n = 8). D, The mRNA levels of *atrogin-1* and *MuRF-1* in the lysates of gastrocnemius muscle from the saline/DW (1.0 ± 0.17, 1.0 ± 0.10; n = 8), BLM/DW (2.27 ± 0.58, 3.70 ± 1.02; n = 7), and BLM/RKT (0.98 ± 0.14, 1.34 ± 0.34; n = 8) groups 14 days after BLM or saline treatment. Values are expressed as means ± SEM relative to saline/DW controls, analyzed by 1-way ANOVA and then Dunnett multiple comparison test. *P < .05; **P < .01.

RKT did not decrease the degree of weight loss and food intake reduction in both *ghrelin*$^{-/-}$ and *Ghsr*$^{-/-}$ mice, after BLM injection. These findings suggest that RKT administration exerts protective effects on the retention of feeding and body weight through the ghrelin system in BLM-injected mice. The antifibrotic effects of RKT might also indirectly contribute to mitigate food intake reduction and body weight loss through the improvement of respiratory status in BLM-injected mice.

Rikkunshito administration mitigated skeletal muscle wasting in mice with BLM-induced lung fibrosis. Skeletal muscle atrophy is an important prognosis factor in patients with pulmonary cachexia [30]. With the progression of skeletal muscle atrophy, the local production of IGF-1 in skeletal muscle is inhibited [32], and the expressions of *atrogin-1* and *MuRF-1*, which are muscle-specific E3 ubiquitin ligases that promote the degradation of proteins, were augmented [33]. Ghrelin is reported to increase the local production of IGF-1 [34], to inhibit the expressions of *atrogin-1* and *MuRF-1*[12,34], and to suppress muscle atrophy [12,34]. In the present study, we demonstrated increased mRNA expressions of *atrogin-1* and *MuRF-1* mRNA in mice with BLM-induced lung fibrosis. The increases of these parameters were inhibited by RKT administration with a restoration of skeletal muscle wasting. Rikkunshito administration may exert protective effects against skeletal muscle wasting through its promotion of the activity of ghrelin expression.

The administration of the 5HT2B receptor antagonist inhibited the decrease of the plasma ghrelin level and the reduction of food intake in BLM-injected mice. Serotonin 2B receptors are distributed in the glandular stomach, and the stimulation of these receptors is reported to reduce food intake [35]. A previous study demonstrated that ghrelin secretion from the gastric mucosa was inhibited by the stimulation of 5HT2B receptors [36]. Another study showed that some of the flavonoids contained in RKT, such as heptamethoxyflavone, isoliquiritigenin, and hesperidin, had antagonistic effects on 5HT2B receptor [23], and the administrations of these flavonoids suppressed the reduction of

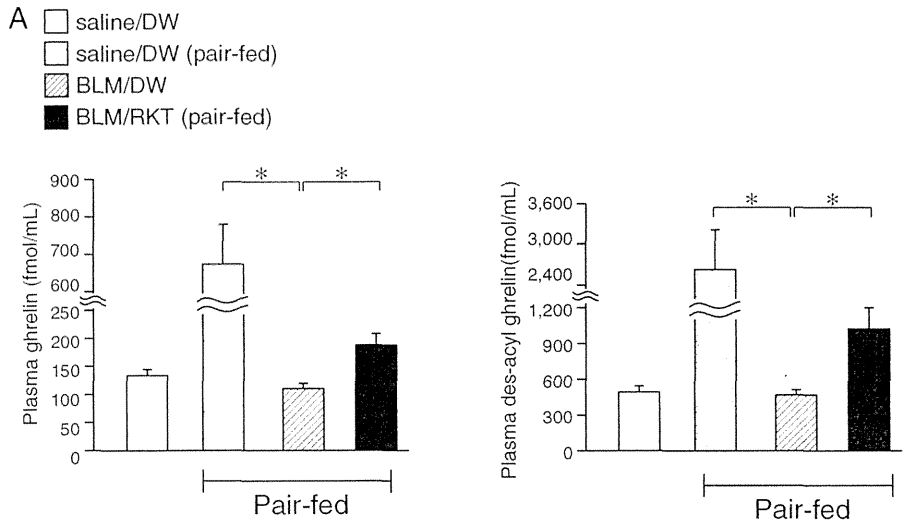

Fig. 4 – Effects of RKT administration on the plasma levels of ghrelin and des-acyl ghrelin in BLM-injected mice. The respective plasma levels of ghrelin and des-acyl ghrelin of the DW (133.7 ± 7.9 fmol/mL, 497.0 ± 28.2 fmol/mL; n = 10), the saline/DW pair-fed (667.9 ± 174.7 fmol/mL, 2626.0 ± 584.4 fmol/mL; n = 10), the BLM/DW (109.2 ± 6.6 fmol/mL, 472.5 ± 18.3 fmol/mL; n = 10), and the BLM/RKT pair-fed group (188.1 ± 18.4 fmol/mL, 1003.3 ± 172.4 fmol/mL; n = 10). The BLM/RKT pair-fed group and saline/DW pair-fed group were fed the same quantity of diet as that consumed by animals of the BLM/DW group. Control group: saline/DW. Data are means ± SEM, analyzed by 1-way ANOVA and then Dunnett multiple comparison test. *P < .05.

plasma ghrelin levels in cisplatin-treated rats [23]. Therefore, the effect of RKT on the induction of plasma ghrelin might be, at least in part, mediated by its antagonistic activity against 5HT2B receptors. This is supported by a recent report stating that an administration of 5HT2B receptor antagonist, as well as that of RKT, mitigated food intake reduction associated with a novelty stress model in mice [37].

Previously, we found that ghrelin administration led to the alleviation of decreased food intake in a murine model of lung fibrosis [17]. In that study, a large amount of exogenous

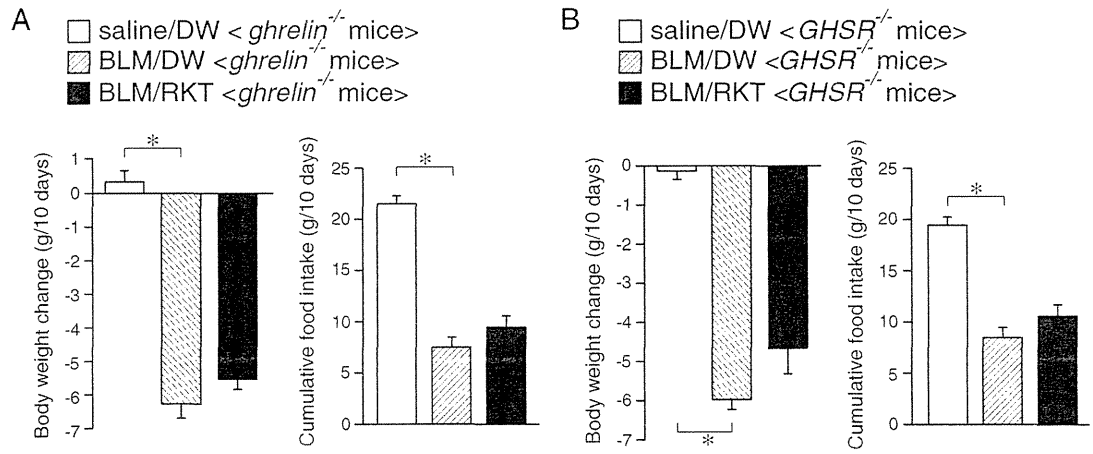

Fig. 5 – Effects of RKT administration on food intake and weight change in BLM-injected, ghrelin-deficient mice and BLM-injected, growth hormone secretagogue receptor–deficient mice. A, Alterations in body weight and cumulative food intake for 10 days after the instillation of 3.0 mg/kg of BLM or saline in ghrelin-deficient (*ghrelin*$^{-/-}$) mice. Saline/DW (body weight change 0.3 ± 0.3 g, cumulative food intake 21.4 ± 1.0 g; n = 6), BLM/DW (–6.3 ± 0.4 g, 7.5 ± 0.9 g; n = 13), and BLM/RKT (–5.5 ± 0.3 g, 9.5 ± 0.8 g; n = 11). B, Alterations in body weight and cumulative food intake for 7 days after the instillation of 3.0 mg/kg of BLM or saline in the growth hormone secretagogue receptor–deficient (*Ghsr*$^{-/-}$) mice. Saline/DW (body weight change 0.0 ± 0.3 g, cumulative food intake 19.5 ± 0.8 g; n = 8), BLM/DW (–5.9 ± 0.4 g, 8.9 ± 0.6 g; n = 7), and BLM/RKT (–4.6 ± 0.6 g, 10.6 ± 1.2 g; n = 8). Control group: saline/DW. Data are means ± SEM, analyzed by 1-way ANOVA and then Dunnett multiple comparison test. *P < .05.

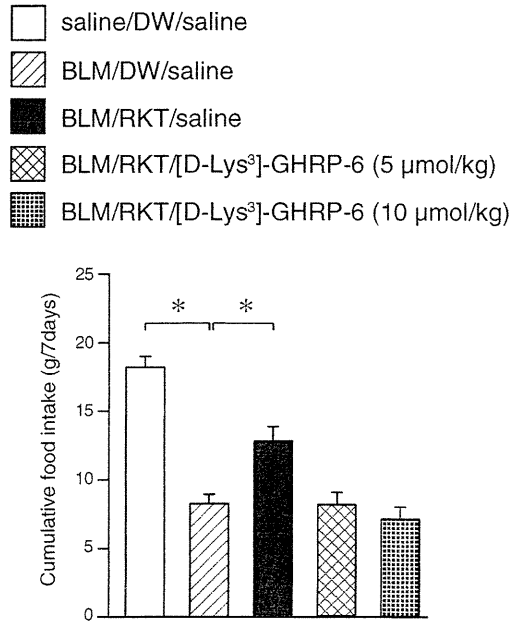

Fig. 6 – Effects of RKT administration on food intake in BLM-injected, growth hormone secretagogue receptor antagonist-treated mice. Cumulative food intake in the saline/DW/saline group (22.3 ± 0.6 g, n = 19), BLM/DW/saline group (10.8 ± 0.7 g, n = 16), BLM/RKT/saline group (16.2 ± 1.3 g, n = 13), BLM/RKT/[D-Lys^3]-GHRP-6 5 μmol/kg group (11.6 ± 1.0 g, n = 19), and the BLM/RKT/[D-Lys^3]-GHRP-6 10 μmol/kg group (10.3 ± 0.9 g, n = 16) for 7 days after BLM or saline treatment. Rikkunshito or DW was administered orally, starting 3 days before the BLM administration during the study interval. [D-Lys^3]-GHRP-6 (5 or 10 μmol/kg) dissolved in saline or saline alone was intraperitoneally administered daily over the 7-day interval starting 1 day after BLM injection. Control group: saline/DW/saline. Data are means ± SEM, analyzed by 1-way ANOVA and then Dunnett multiple comparison test. *P < .05.

ghrelin was necessary to increase the food intake in BLM-injected mice [17]. Therefore, with regard to the increase in food intake, mice with BLM-induced lung fibrosis may be resistant to ghrelin stimulation. In vitro studies have shown that RKT and its constituent compounds, atractylodin and atractylodinol, enhanced the binding activity of ghrelin to the growth hormone secretagogue receptor and also sustained the ghrelin-induced cytosolic Ca^{2+} concentration increase in growth hormone secretagogue receptor–expressing cells [16]. The orexigenic effect of peripheral ghrelin depends on the vagal afferent activity mediated by an interaction with ghrelin and GHS-R1a, which is expressed at vagal afferent terminals [38]. Thus, RKT might increase food intake in BLM-injected mice by intensifying transduction of ghrelin signals to the brain via the afferent vagal nerve through the up-regulation of the binding activity of ghrelin to GHS-R1a. Supporting this idea, our previous study revealed that although RKT mitigated weight loss and decrease of food intake in BLM-injected mice, the plasma ghrelin levels of RKT-administered, BLM-injected mice were significantly lower when compared with the levels in BLM-injected mice that were administered a pharmacologic dose of ghrelin [17,18].

There are some important methodological limitations in this study. First, the model of BLM-induced lung fibrosis is not completely relevant to the clinical manifestation of lung fibrosis. The intratracheal injection of BLM induces an inflammatory cell infiltration in the lung parenchyma before the development of lung fibrosis [21]. In addition, although clinical presentations of lung fibrosis are progressive, BLM-induced lung fibrosis may be self-limiting 28 days after the BLM injection [21]. Second, there are differences in RKT between clinical doses and the experimental dose used in this study. The standard prescribed dose of RKT in patients with gastric symptoms is 7500 mg/d (approximately 150 mg kg^{-1} d^{-1} in a person weighing 50 kg) [15]. In the present experiments, we used a higher dosage (1000 mg kg^{-1} d^{-1}) of RKT, compared with the standard prescribed dosage. Because a low dosage (500 mg kg^{-1} d^{-1}) of RKT did not mitigate the body weight reduction but a high dosage (1000 mg kg^{-1} d^{-1}) of RKT did mitigate it in BLM-injected mice [18], we set the experimental dosage of RKT at 1000 mg kg^{-1} d^{-1}. Third, it is not yet known which components of RKT are effective against pulmonary cachexia. Among the metabolites derived from RKT components, 8-prenylnaringenin was reported to prevent disuse muscle atrophy in denervated mice [39], and isoliquiritigenin was reported to attenuate food intake reduction in novelty stress model mice [37]. Further studies should be conducted to identify the RKT components that contribute to the relief of muscle wasting and food intake reduction as well as their precise mechanisms.

In summary, our results demonstrated the efficacy of RKT administration in a rodent model of pulmonary cachexia associated with lung fibrosis. Rikkunshito administration did not mitigate reduction of food intake or decrease of body weight in *ghrelin*$^{-/-}$ mice, *Ghsr*$^{-/-}$ mice, or ghrelin receptor antagonist-treated WT mice under the conditions of lung fibrosis. These findings support our initial hypotheses that RKT administration exerts protective effects on pulmonary cachexia by mitigating skeletal muscle wasting and food intake reduction, dependent of the ghrelin system. The results highlight RKT as a potential therapeutic agent for the management of this intractable disease.

Acknowledgment

We thank Koji Toshinai, Sumie Tajiri, and Miki Oshikawa (Miyazaki University) for their technical support. This work was supported, in part, by a Grant-in-Aid for Scientific Research (No. 24591171); a Grant-in-Aid for challenging Exploratory Research (No. 24659406); a grant from the Ministry of Education, Culture, Sports, Science, and Technology; a Health and Labour Sciences Research Grant for Clinical Research Translational Research General (No. 002); a grant from the Japan Intractable Diseases Research Foundation; and a grant from Tsumura and Co. S.I., S.M., C.Y., and T.H. are employed by Tsumura & Co. H.T., S.Y., A.M., and M.N. have no conflicts to declare.

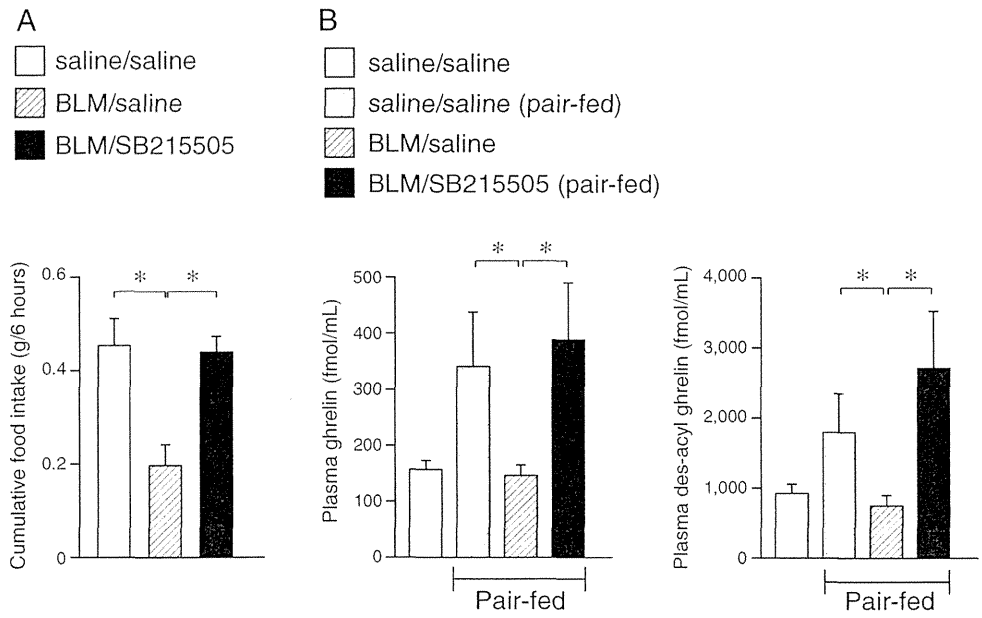

Fig. 7 – Effect of 5HT2B receptor antagonist on food intake and the plasma levels of ghrelin and des-acyl ghrelin in BLM-injected mice. A, Cumulative food intake (6 hours) in the saline/saline group (0.46 ± 0.06 g, n = 10), BLM/saline group (0.20 ± 0.03 g, n = 10), and BLM/SB215505 group (0.44 ± 0.03 g, n = 10) 5 days after the BLM or saline injection. Control group: the saline/saline group. B, Plasma levels of ghrelin and des-acyl ghrelin of the saline/saline group (ghrelin 156.6 ± 11.0 fmol/mL, des-acyl ghrelin 935.6 ± 58.2 fmol/mL; n = 10), saline/saline pair-fed group (336.6 ± 103.0 fmol/mL, 1821.6 ± 542 fmol/mL; n = 10), BLM/saline group (143.5 ± 9.5 fmol/mL, 756.5 ± 87.9 fmol/mL; n = 10), and BLM/SB215505 pair-fed group (384.0 ± 105.2 fmol/mL, 2721.3 ± 826.0 fmol/mL; n = 10). The BLM/SB215505 pair-fed group and saline/saline pair-fed group were fed the same quantity of diet as that consumed by animals of the BLM/saline group. Control group: saline/saline. Data are means ± SEM, analyzed by 1-way ANOVA and then Dunnett multiple comparison test. *P < .05.

REFERENCES

[1] Fearon KC, Glass DJ, Guttridge DC. Cancer cachexia: mediators, signaling, and metabolic pathways. Cell Metab 2012;16:153–66.

[2] Remels AH, Gosker HR, Langen RC, Schols AM. The mechanisms of cachexia underlying muscle dysfunction in COPD. J Appl Physiol 2013;114:1253–62.

[3] Nishimura K, Izumi T, Tsukino M, Oga T. Dyspnea is a better predictor of 5-year survival than airway obstruction in patients with COPD. Chest 2002;121:1434–40.

[4] Nishiyama O, Taniguchi H, Kondoh Y, Kimura T, Kato K, Kataoka K, et al. A simple assessment of dyspnoea as a prognostic indicator in idiopathic pulmonary fibrosis. Eur Respir J 2010;36:1067–72.

[5] Fitting JW, Frascarolo P, Jequier E, Leuenberger P. Resting energy expenditure in interstitial lung disease. Am Rev Respir Dis 1990;142:631–5.

[6] Ramires BR, de Oliveira EP, Pimentel GD, McLellan KC, Nakato DM, Faganello MM, et al. Resting energy expenditure and carbohydrate oxidation are higher in elderly patients with COPD: a case control study. Nutr J 2012;11:37.

[7] Swallow EB, Reyes D, Hopkinson NS, Man WD, Porcher R, Cetti EJ, et al. Quadriceps strength predicts mortality in patients with moderate to severe chronic obstructive pulmonary disease. Thorax 2007;62:115–20.

[8] Alakhras M, Decker PA, Nadrous HF, Collazo-Clavell M, Ryu JH. Body mass index and mortality in patients with idiopathic pulmonary fibrosis. Chest 2007;131:1448–53.

[9] Cano NJ, Pichard C, Roth H, Court-Fortune I, Cynober L, Gerard-Boncompain M, et al. C-reactive protein and body mass index predict outcome in end-stage respiratory failure. Chest 2004;126:540–6.

[10] Kojima M, Hosoda H, Date Y, Nakazato M, Matsuo H, Kangawa K. Ghrelin is a growth-hormone–releasing acylated peptide from stomach. Nature 1999;402:656–60.

[11] Nakazato M, Murakami N, Date Y, Kojima M, Matsuo H, Kangawa K, et al. A role for ghrelin in the central regulation of feeding. Nature 2001;409:194–8.

[12] Porporato PE, Filigheddu N, Reano S, Ferrara M, Angelino E, Gnocchi VF, et al. Acylated and unacylated ghrelin impair skeletal muscle atrophy in mice. J Clin Invest 2013;123:611–22.

[13] Nagaya N, Itoh T, Murakami S, Oya H, Uematsu M, Miyatake K, et al. Treatment of cachexia with ghrelin in patients with COPD. Chest 2005;128:1187–93.

[14] Yagi M, Homma S, Kubota M, Iinuma Y, Kanada S, Kinoshita Y, et al. The herbal medicine Rikkunshi-to stimulates and coordinates the gastric myoelectric activity in post-operative dyspeptic children after gastrointestinal surgery. Pediatr Surg Int 2004;19:760–5.

[15] Arai M, Matsumura T, Tsuchiya N, Sadakane C, Inami R, Suzuki T, et al. Rikkunshito improves the symptoms in patients with functional dyspepsia, accompanied by an increase in the level of plasma ghrelin. Hepatogastroenterology 2012;59:62–6.

[16] Fujitsuka N, Asakawa A, Uezono Y, Minami K, Yamaguchi T, Niijima A, et al. Potentiation of ghrelin signaling attenuates cancer anorexia-cachexia and prolongs survival. Transl Psychiatry 2011;1.e23.

[17] Imazu Y, Yanagi S, Miyoshi K, Tsubouchi H, Yamashita S, Matsumoto N, et al. Ghrelin ameliorates bleomycin-induced acute lung injury by protecting alveolar epithelial cells and suppressing lung inflammation. Eur J Pharmacol 2011;672:153–8.
[18] Tsubouchi H, Yanagi S, Miura A, Iizuka S, Mogami S, Yamada C, et al. Rikkunshito ameliorates bleomycin-induced acute lung injury in a ghrelin-independent manner. Am J Physiol Lung Cell Mol Physiol 2014;306:L233–45.
[19] Sato T, Kurokawa M, Nakashima Y, Ida T, Takahashi T, Fukue Y, et al. Ghrelin deficiency does not influence feeding performance. Regul Pept 2008;145:7–11.
[20] Sun Y, Wang P, Zheng H, Smith RG. Ghrelin stimulation of growth hormone release and appetite is mediated through the growth hormone secretagogue receptor. Proc Natl Acad Sci U S A 2004;101:4679–84.
[21] Moore BB, Hogaboam CM. Murine models of pulmonary fibrosis. Am J Physiol Lung Cell Mol Physiol 2008;294:L152–60.
[22] Chambers AP, Wilson-Perez HE, McGrath S, Grayson BE, Ryan KK, D'Alessio DA, et al. Effect of vertical sleeve gastrectomy on food selection and satiation in rats. Am J Physiol Endocrinol Metab 2012;303:E1076–84.
[23] Takeda H, Sadakane C, Hattori T, Katsurada T, Ohkawara T, Nagai K, et al. Rikkunshito, an herbal medicine, suppresses cisplatin-induced anorexia in rats via 5-HT2 receptor antagonism. Gastroenterology 2008;134:2004–13.
[24] Zhang G, Jin B, Li YP. C/EBPbeta mediates tumour-induced ubiquitin ligase atrogin1/MAFbx upregulation and muscle wasting. EMBO J 2011;30:4323–35.
[25] Cao P, Hanai J, Tanksale P, Imamura S, Sukhatme VP, Lecker SH. Statin-induced muscle damage and atrogin-1 induction is the result of a geranylgeranylation defect. FASEB J 2009;23:2844–54.
[26] Faul F, Erdfelder E, Lang AG, Buchner A. G*Power 3: a flexible statistical power analysis program for the social, behavioral, and biomedical sciences. Behav Res Methods 2007;39:175–91.
[27] Skeletal muscle dysfunction in chronic obstructive pulmonary disease. A statement of the American Thoracic Society and European Respiratory Society. Am J Respir Crit Care Med 1999;159:S1–S40.
[28] Mendoza L, Gogali A, Shrikrishna D, Cavada G, Kemp SV, Natanek SA, et al. Quadriceps strength and endurance in fibrotic idiopathic interstitial pneumonia. Respirology 2014; 19:138–43.
[29] Prescott E, Almdal T, Mikkelsen KL, Tofteng CL, Vestbo J, Lange P. Prognostic value of weight change in chronic obstructive pulmonary disease: results from the Copenhagen City Heart Study. Eur Respir J 2002;20:539–44.
[30] Marquis K, Debigare R, Lacasse Y, LeBlanc P, Jobin J, Carrier G, et al. Midthigh muscle cross-sectional area is a better predictor of mortality than body mass index in patients with chronic obstructive pulmonary disease. Am J Respir Crit Care Med 2002;166:809–13.
[31] Asakawa A, Inui A, Kaga T, Katsuura G, Fujimiya M, Fujino MA, et al. Antagonism of ghrelin receptor reduces food intake and body weight gain in mice. Gut 2003;52:947–52.
[32] Costelli P, Muscaritoli M, Bossola M, Penna F, Reffo P, Bonetto A, et al. IGF-1 is downregulated in experimental cancer cachexia. Am J Physiol Regul Integr Comp Physiol 2006;291: R674–83.
[33] Foletta VC, White LJ, Larsen AE, Leger B, Russell AP. The role and regulation of MAFbx/atrogin-1 and MuRF1 in skeletal muscle atrophy. Pflugers Arch 2011;461:325–35.
[34] Sugiyama M, Yamaki A, Furuya M, Inomata N, Minamitake Y, Ohsuye K, et al. Ghrelin improves body weight loss and skeletal muscle catabolism associated with angiotensin II–induced cachexia in mice. Regul Pept 2012;178:21–8.
[35] Hattori T, Yakabi K, Takeda H. Cisplatin-induced anorexia and ghrelin. Vitam Horm 2013;92:301–17.
[36] Takeda H, Nakagawa K, Okubo N, Nishimura M, Muto S, Ohnishi S, et al. Pathophysiologic basis of anorexia: focus on the interaction between ghrelin dynamics and the serotonergic system. Biol Pharm Bull 2013;36:1401–5.
[37] Yamada C, Saegusa Y, Nakagawa K, Ohnishi S, Muto S, Nahata M, et al. Rikkunshito, a Japanese kampo medicine, ameliorates decreased feeding behavior via ghrelin and serotonin 2B receptor signaling in a novelty stress murine model. Biomed Res Int 2013;2013:792940.
[38] Date Y, Murakami N, Toshinai K, Matsukura S, Niijima A, Matsuo H, et al. The role of the gastric afferent vagal nerve in ghrelin-induced feeding and growth hormone secretion in rats. Gastroenterology 2002;123:1120–8.
[39] Mukai R, Horikawa H, Fujikura Y, Kawamura T, Nemoto H, Nikawa T, et al. Prevention of disuse muscle atrophy by dietary ingestion of 8-prenylnaringenin in denervated mice. PLoS One 2012;7:e45048.

European Journal of Pharmacology 743 (2014) 1–10

Contents lists available at ScienceDirect

European Journal of Pharmacology

journal homepage: www.elsevier.com/locate/ejphar

Pulmonary, gastrointestinal and urogenital pharmacology

Ghrelin relieves cancer cachexia associated with the development of lung *adenocarcinoma in mice*

Hironobu Tsubouchi [a], Shigehisa Yanagi [a], Ayako Miura [a], Nobuhiro Matsumoto [a], Kenji Kangawa [b], Masamitsu Nakazato [a,*]

[a] Division of Neurology, Respirology, Endocrinology and Metabolism, Department of Internal Medicine, Faculty of Medicine, University of Miyazaki, Kiyotake, Miyazaki 889-1692, Japan
[b] Department of Biochemistry, National Cardiovascular Center Research Institute, 5-7-1 Fujishiro-dai, Suita, Osaka 565-8565, Japan

ARTICLE INFO

Article history:
Received 15 October 2013
Received in revised form
16 September 2014
Accepted 16 September 2014
Available online 23 September 2014

Keywords:
Ghrelin
Cancer
Cachexia
Muscle atrophy

ABSTRACT

Cancer cachexia is a multifactorial, critical illness syndrome characterized by an ongoing loss of skeletal muscle and adipose tissue. The reductions in body weight and skeletal muscle mass are important prognostic indicators for cancer patients that are refractory to current therapies. Ghrelin, an endogenous ligand for the growth hormone secretagogue receptor, is produced in the stomach, stimulates food intake and growth hormone secretion, suppresses inflammation, and prevents muscle catabolism. We investigated the pharmacological potential of ghrelin in the treatment of cancer cachexia by using urethane-treated, bronchioalveolar epithelium-specific *Pten*-deficient mice that developed lung adenocarcinomas. Ghrelin or phosphate-buffered saline was given to mice daily for four weeks beginning at five months after urethane injection, which corresponded to the time point of lung adenocarcinoma formation. Ghrelin inhibited the inductions of C-reactive protein, tumor necrosis factor-α, interleukin-1β, and interleukin-6, mitigated the reduction of food intake and fat mass, and consequently ameliorated body weight loss in the mouse model of lung adenocarcinoma. We also demonstrated that skeletal muscle mass and muscle contraction force in both fast-twitch muscle and slow-twitch muscle were retained in ghrelin-treated mice in conjunction with an upregulation of local insulin-like growth factor 1/Akt signaling. In addition, ghrelin administration reduced the expressions of phosphorylated-p38 mitogen-activated protein kinase, phosphorylated-nuclear factor-kappa B, Forkhead box protein O1, muscle RING-finger protein-1, and F-Box protein 32 in the lysates of skeletal muscle in the tumor-bearing state. Our results indicate that ghrelin administration exerts a protective effect against cancer cachexia by ameliorating skeletal muscle wasting and regulating systemic inflammation.

1. Introduction

Cancer cachexia affects up to 80% of patients with advanced cancers and accounts for nearly 30% of cancer-related deaths (Acharyya et al., 2005; Fearon, 2008). A key feature of cachexia is significant reduction in body weight resulting predominantly from progressive depletion of skeletal muscle mass (Fearon et al., 2012). Muscle atrophy leads to general muscle weakness, impairment of activity of daily life, and eventually death through respiratory failure. The mechanisms of cancer cachexia are multifactorial, and cannot be fully reversed by nutritional support alone. Various hormones, proinflammatory cytokines, and tumor-derived factors have been shown to influence muscle protein synthesis/degradation balance through several major intracellular signal-transduction systems, including the insulin-like growth factor 1 (IGF1)/insulin receptor substrate 1/Akt pathway and the Forkhead box protein O1 (FoxO1)/muscle RING-finger protein-1 (MuRF1)/F-Box protein-32 (Atrogin1) pathway (Zhou et al., 2010). Ideal interventions against cancer cachexia should exert their effects both upstream (antagonizing key mediators of systemic inflammation) and downstream (blocking catabolic pathways or stimulating anabolic pathways in skeletal muscle) (Fearon et al., 2012). Despite recent advances in understanding the pathological mechanisms of cancer cachexia, few therapeutic options are currently available. In addition, there is no ideal rodent cancer cachexia model for replicating the condition in humans.

Ghrelin is a 28-amino-acid peptide initially isolated from the human and rat stomach as an endogenous ligand for the growth hormone secretagogue (GHS)-receptor (Kojima et al., 1999). While ghrelin has a potent orexigenic effect independently of growth hormone (GH) secretion, ghrelin is also known to have multifaceted effects on energy metabolism, including decrease of energy expenditure (Yasuda et al., 2003), stimulation of adiposity (Tschop et al., 2000),

* Corresponding author. Tel.: +81 985 85 2965; fax: +81 985 85 1869.
E-mail address: nakazato@med.miyazaki-u.ac.jp (M. Nakazato).

http://dx.doi.org/10.1016/j.ejphar.2014.09.025
0014-2999/

and prevention of muscle catabolism (Koshinaka et al., 2011; Sugiyama et al., 2012). In addition, ghrelin inhibits the expression of proinflammatory anorectic cytokines in human monocytes and T cells (Dixit et al., 2004). These observations suggest that ghrelin might improve cachectic conditions. Previous studies using tumor implantation models have reported that ghrelin administration resulted in significant increases in food intake and body weight (DeBoer et al., 2007; Hanada et al., 2003). However, the therapeutic effect and molecular mechanisms of ghrelin treatment against cancer cachexia, including muscle wasting, remain unknown, especially in the context of a model of cancer development.

We previously reported that almost all mice with a bronchioalveolar epithelium-specific null mutation of *Pten*, a tumor suppressor gene mutated in many human cancers, including lung adenocarcinoma (Marsit et al., 2005; Tang et al., 2006), spontaneously developed lung adenocarcinomas (Yanagi et al., 2007). This animal model of lung adenocarcinoma is highly reproducible and accelerates cancer formation over a relatively short time course by administration of urethane, a well-known initiator of lung carcinomas (Malkinson and Beer, 1983). In this study, we showed that there were marked upregulations of markers of muscle atrophy and proinflammatory cytokines as well as significant reduction in body weight and loss of skeletal muscle mass in urethane-treated, bronchioalveolar epithelium-specific *Pten*-deficient mice. To investigate the efficacy of ghrelin treatment against the syndrome of cancer cachexia in the present study, we used this mouse model of lung adenocarcinoma.

2. Materials and methods

2.1. Animals and administration of doxycycline

We generated bronchioalveolar epithelial cell-specific *Pten*-deficient mice as previously described (Yanagi et al., 2007). Briefly, $Pten^{flox/flox}$ mice (129Ola × C57BL6/J F6) generated as described in an earlier study (Suzuki et al., 2001) were mated to *SP-C-rtTA* mice (Perl et al., 2002) that express the reverse tetracycline-controlled transactivator (rtTA) gene (which can be activated by doxycycline) under the control of the 3.7-kb human surfactant protein-C (SP-C) promoter (Perl et al., 2002). The human SP-C promoter selectively directs expression of the transgene to the developing and the mature pulmonary epithelium of the primordial lung buds, and to bronchiolar epithelial cells and type II alveolar epithelial cells after birth (Wert et al., 1993). Triple transgenic mice were generated by mating *SP-C-rtTA/*$Pten^{flox/flox}$ mice with $(tetO)_7$*-Cre* mice (Sauer, 1998) that express Cre recombinase under the control of rtTA. Unless otherwise noted, offspring carrying *SP-C-rtTA/*$(tetO)_7$*-Cre/*$Pten^{flox/flox}$ ($SOPten^{f/f}$) and their littermates carrying $(tetO)_7$*-Cre/*$Pten^{flox/flox}$ ($OPten^{f/f}$) were used in the experiments as homozygous mutant and wild-type mice, respectively. To induce expression of the *Cre* transgene in bronchioalveolar epithelial cells postnatally, 3-week-old mice (P21) were administered doxycycline (Sigma-Aldrich Japan, Tokyo) in their drinking water (1 mg/ml) for 1 week. After administration of doxycycline, $SOPten^{f/f}$ mice, which were fed doxycycline from P21 to P27, were designated as $SOPten^{\Delta/\Delta}$ mice. Mice were housed in a temperature-controlled room (23 ± 1 °C) on a 12-h light (08:00–20:00 h)/12-h dark cycle and fed a standard laboratory chow with ad libitum access to food. All experimental procedures were performed in accordance with the Japanese Physiological Society's guidelines for animal care and were approved by the Ethics Committee on Animal Experimentation of the University of Miyazaki.

2.2. Lung carcinogenesis

The 8-week-old $SOPten^{\Delta/\Delta}$ and $OPten^{f/f}$ mice were intraperitoneally administered 1 g/kg of urethane (Sigma-Aldrich Japan, Tokyo) which was dissolved in 200 μl phosphate buffered saline (PBS). For the survival study ($SOPten^{\Delta/\Delta}$ mice, $n=28$; and $OPten^{f/f}$ mice, $n=25$), the measurements of body weights ($SOPten^{\Delta/\Delta}$ mice, $n=15$; and $OPten^{f/f}$ mice, $n=24$), and the histological assay ($SOPten^{\Delta/\Delta}$ mice, $n=10$; and $OPten^{f/f}$ mice, $n=10$), we used male 8-week-old $SOPten^{\Delta/\Delta}$ and $OPten^{f/f}$ mice, and monitored them for 30 weeks.

2.3. Administration of ghrelin

At the age of 38 weeks, the urethane-injected $SOPten^{\Delta/\Delta}$ mice were intraperitoneally administered 10 nmol/mouse of human ghrelin (Asubio Pharma Co., Kobe, Japan) dissolved in 200 μl PBS or PBS alone at 07:00 and 19:00 over a 28-day interval. The 38-week-old, urethane-injected $OPten^{f/f}$ mice were given PBS intraperitoneally during the 28-day study interval. On 28 days after administration of ghrelin or PBS, mice were anesthetized by intraperitoneal injection of pentobarbital sodium and sacrificed. We then designated the ghrelin-treated, urethane-injected $SOPten^{\Delta/\Delta}$ mice as the $SOPten^{\Delta/\Delta}$/ghrelin group, the PBS-treated, urethane-injected $SOPten^{\Delta/\Delta}$ mice as the $SOPten^{\Delta/\Delta}$/PBS group, and the PBS-treated, urethane-injected $OPten^{f/f}$ mice as the $OPten^{f/f}$/PBS group. Body weights and food intake were measured daily from 1 day before ghrelin or PBS administration to day 28. We used the animals from the $SOPten^{\Delta/\Delta}$/ghrelin group, $SOPten^{\Delta/\Delta}$/PBS group and $OPten^{f/f}$/PBS group for the measurements of body weights and food intake ($n=12$–13 per group). For the measurements of skeletal muscle mass (gastrocnemius: $n=12$–23 per group; tibialis anterior muscle: $n=12$–13 per group; and soleus muscle: $n=12$–13 per group), the measurements of muscle contraction force ($n=6$–8 per group), the measurements of intra-abdominal fat mass ($n=12$–23 per group), the enzyme-linked immunosorbent assay (ELISA) ($n=8$–15 per group), the quantitative real-time PCR ($n=5$–7 per group), the immunohistochemical analyses ($n=5$ per group), and the Western blotting ($n=3$ per group), we used three

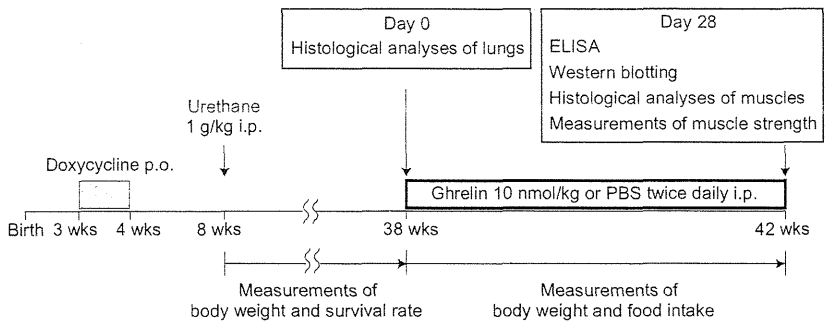

Fig. 1. Timeline of doxycycline, urethane, and ghrelin treatment in $OPten^{f/f}$ and $SOPten^{\Delta/\Delta}$ mice. PBS, phosphate buffered saline; ELSIA, enzyme-linked immunosorbent assay.

additional groups and examined the animals on day 28. The experimental protocol of the study is outlined in Fig. 1.

2.4. Measurement of plasma ghrelin levels

The 10-week-old *OPten*$^{f/f}$ mice were intraperitoneally administered 1 or 10 nmol/mouse of human ghrelin (Asubio Pharma Co., Kobe, Japan) dissolved in 200 μl PBS or PBS alone. At 2, 3, or 12 h after the ghrelin or PBS injection, blood was taken from the mice by heart puncture and collected in a tube which contained aprotinin and ethylenediaminetetraacetic acid (Wako, Osaka, Japan). The contents were mixed well and immediately centrifuged at 4 °C. After plasma collection, a 1/10 volume of 1 mol/L HCl was added. The prepared plasma was stored at −80 °C until the measurement of ghrelin. The plasma ghrelin assay is a two-site immunoenzymometric assay requiring 100 μl of plasma sample, which is performed automatically by an AIA-600II immunoassay analyzer (Tosoh Corp., Tokyo, Japan).

2.5. Measurement of plasma cytokine levels, C-reactive protein, and IGF1

An ELISA was run using the plasma samples to measure the concentrations of C-reactive protein (Life Diagnostics Inc., West Chester, NY), interleukin-6 (IL-6), interleukin-1β (IL-1β), tumor necrosis factor-α (TNF-α), and IGF1 by using the commercially available ELISA kits specifically designed for each protein (R&D Systems, Minneapolis, MN) according to the manufacturer's instructions.

2.6. Histological analyses

The lungs and gastrocnemius muscles were fixed in 10% buffered formalin solution and embedded in optimum cutting temperature compound (Sakura Finetek Japan, Tokyo). Lung sections (4 μm thickness) and muscles (6 μm thickness) were mounted on slides for hematoxylin-eosin (HE) staining or immunostaining with an antibody recognizing laminin (Sigma-Aldrich Japan, Tokyo). For each muscle section, the whole muscle cross section was analyzed to calculate the average fiber size (cross-section area) by using the program Image J 1.46 (freeware developed by Dr. W. Rasband at the Research Services Branch, National Institute of Mental Health, and available at http://rsb.info.nih.gov/ij). The cross section areas of muscle sections from 5 mice per group were quantified by using the Image J software. The mean of the cross section area was calculated based on measurements of 229–370 myofibers per mouse.

2.7. Measurements of the contractile force of skeletal muscles

For measurements of the contractile force of skeletal muscles in the *SOPten*$^{\Delta/\Delta}$/ghrelin group, *SOPten*$^{\Delta/\Delta}$/PBS group and *OPten*$^{f/f}$/PBS group, mice were anesthetized at day 28 of ghrelin or PBS treatment. After exteriorization of the right soleus muscle or right tibialis anterior muscle and the right sciatic nerve, the Achilles tendon or tendon of the tibialis anterior was cut and connected to a muscle force-measuring device, the MLTF500/ST Teaching force transducer (ADInstruments Japan, Nagoya, Japan). For the measurements of the twitching contractile force or tetanic contractile force, the dominant nerve of muscles was electrically stimulated with 5 mA/1 Hz (duration: 10 s; pulse width: 0.1 ms) or 5 mA/75 Hz (duration: 5 s; pulse width: 0.1 ms), respectively, by an FE180 Stimulus isolator (ADInstruments Japan). The maximal contractile forces under fast-twitching stimulation or tetanic stimulation were analyzed by a ML846 PowerLab 4/26 system (ADInstruments Japan).

2.8. Extraction of mRNA and quantitative real-time PCR

We measured the mRNA expressions of atrogin-1, MuRF-1, and IGF1 in the gastrocnemius muscles of the *SOPten*$^{\Delta/\Delta}$/ghrelin group, *SOPten*$^{\Delta/\Delta}$/PBS group and *OPten*$^{f/f}$/PBS group at day 28 of ghrelin or PBS treatment. The mRNA was extracted from the whole gastrocnemius muscle using a Ribopure™ Kit (Life Technologies Japan Inc., Tokyo, Japan). First-strand cDNA was generated by reverse transcription using a High Capacity RNA-to-cDNA Kit (Life Technologies Japan Inc.). Quantitative real-time PCR was performed using Taqman Fast Universal PCR Master Mix (Life Technologies Japan Inc.) and a Thermal Cycler Dice Real Time System II (Takara Bio Inc., Tokyo, Japan). The levels of mRNA were determined by using cataloged primers (Applied Biosystems, Foster City, CA) for mice (Atrogin1: Mm00499523_m1; MuRF1: Mm01185221_m1; and IGF1: Mm00439560_m1). Expression of these genes was normalized to the expression of glyceraldehyde 3-phosphate dehydrogenase (GAPDH) mRNA (Gapdh Mm99999915_g1), and the results were expressed as relative fold differences.

2.9. Western blotting

Western blot analysis on whole gastrocnemius muscle was performed as described previously (Kristensen et al., 2014; Tsubouchi et al., 2014). Briefly, the gastrocnemius muscles were homogenized using a Tissuelyser II (Qiagen, Hilden, Germany). The muscle homogenates were centrifuged at 15,000 rpm for 15 min and the supernatants were stored at −70 °C until used. Total protein contents in supernatants were determined using a Bradford assay. Equal amounts of proteins were fractionated by 10% SDS-PAGE and transferred to Immobilon Transfer Membranes (Merck, Tokyo, Japan). We measured the expression levels of proteins in the lysates of gastrocnemius muscle by Western blotting, using antibodies recognizing the following proteins: β-actin (Sigma-Aldrich Japan), phosphorylated-Akt (Ser473), Akt, phosphorylated-FoxO1 (Ser256), FoxO1, phosphorylated-p38 mitogen-activated protein kinase (MAPK) (Thr180/Thy182), p38 MAPK, and phosphorylated-nuclear factor-kappa B (NF-κB) (Cell Signaling Technology Japan Inc., Tokyo, Japan). To quantify the protein expression, densitometry was performed on the lanes using Gene Tools software (Syngene, Frederick, MD).

2.10. Statistical analysis

All results were expressed as the mean ± S.E.M. Data were analyzed by a Tukey–Kramer honestly significant difference test. A Student's *t*-test analysis was used for the single-parameter comparisons between two groups. Statistical analyses were done with JMP 10 (SAS Institute Japan, Ltd., Tokyo, Japan) and values of $P < 0.05$ were considered statistically significant. Kaplan–Meier survival analysis was performed using Prism 5 (GraphPad Software, La Jolla, CA) and statistical significance was determined by a log-rank test.

3. Results

3.1. Urethane-induced lung carcinogenesis and loss of body weights in lung epithelium-specific Pten-deficient mice

The overall survival rate of *SOPten*$^{\Delta/\Delta}$ mice was significantly lower than that of *OPten*$^{f/f}$ mice 30 weeks after urethane injection (Fig. 2A). The body weights in *SOPten*$^{\Delta/\Delta}$ mice were significantly lower than those of *OPten*$^{f/f}$ mice at 30 weeks after injection (Fig. 2B). As shown in Fig. 2C, all of the *SOPten*$^{\Delta/\Delta}$ mice developed macroscopic lung tumors. Histological examination demonstrated that 9 of the 10 *SOPten*$^{\Delta/\Delta}$ mice developed lung adenocarcinomas